Monitoring the morphodynamics of the Zwin inlet

Interim report
2 years after the extension works

DEPARTMENT
MOBILITY &
PUBLIC
WORKS

www.flandershydraulicsresearch.be

Monitoring the morphodynamics of the Zwin inlet

Interim report:
2 years after the works

Montreuil, A-L.; Dan, S.; Houthuys, R.; Verwaest, T.

Flanders
Hydraulics Research

Flanders
State of the Art

Legal notice

Copyright and citation

Document identification

Customer:	Coastal Division MDK		Ref.:	WL2021R16_089_2	
Keywords (3-5):	Entrance and inlet units; erosion/accretion; hydrodynamics; measurements.				
Knowledge domains:	Hydrodynamics > Current velocities and patterns > In-situ measurements Morphology > Erosion/sedimentation > In-situ measurements				
Text (p.):	44		Appendices (p.):	2	
Confidential:	☒ No		☒ Available online		

Author(s):	Montreuil, A-L., Dan, S.

Control

	Name	Signature
Reviser(s):	Verwaest, T.; Houthuys, R.	Getekend door:Toon Verwaest (Signature Getekend op:2022-01-20 13:04:51 +01:0 Reden:Ik keur dit document goed *Toon Verwaest* Rik Houthuys (Authentication) Digitaal ondertekend door Rik Houthuys (Authentication) DN: c=BE, cn=Rik Houthuys (Authentication), sn=Houthuys, givenName=Rik Jozef, serialNumber=61072742397 Datum: 2022.01.19 09:54:44 +01'00'
Project leader:	Dan, S.	Getekend door:Sebastian Dan (Signature Getekend op:2022-01-21 15:09:13 +01:0 Reden:Ik keur dit document goed *Sebastian Dan* Vlaanderen

Approval

Head of Division:	Bellafkih, K.	Getekend door:Abdelkarim Bellafkih (Sig Getekend op:2022-01-20 12:10:09 +01:0 Reden:Ik keur dit document goed *Abdelkarim Bellafkih*

CERTIFIED **LR** ISO 9001

Abstract

The Zwin is a relatively small tidal inlet connected to the North Sea through a tidal channel. The inlet is flooded twice a day and it is characterized by the presence of intertidal area with sand banks and salt marshes. From August 2016 until the opening of the dyke in February 2019, large intervention works were carried out to reduce the sediment silting and accretion processes by increasing the amount of water flowing in and out of the inlet (i.e. tidal prism). On 4 February 2019, the intertidal area was nearly doubled when the International Dijk was cut and a part of the former Willem-Leopold polder was made intertidal. This project aims to evaluate the effects of the intervention work and to improve our understanding on the morphodynamics of the Zwin. Detailed topographic and hydrodynamic measurements were carried out in the entrance and inland inlet units over the period covering the time before the opening of the dyke which was on 04/02/2019 and up to 1.9 years afterwards. The results indicate significant morphological changes in the entire inlet system where the main channel has become deeper and wider. Also, it has experienced an eastward migration along the entire inlet. Although a high spatial variability is noted in the morphological evolution, with a clear onshore mobility of the sandy bedforms in the channel especially in the entrance inlet, the sediment balance is stable there, suggesting that sand bypass dominates there. In contrast, the inland inlet has lost a significant sediment volume over the monitoring period. It has also experienced two clear morphological trends with accretion at the west side with a vertical gain of the sand bank and bars, while erosion dominates in the middle and at the east side. There, the channel has become deeper and wider. Both trend means a migration of the channel toward the east. Since the interventions, the water discharge during the flood and ebb phase has significantly increased. It is linearly related to the geometrical characteristics of the tidal basin and water level. Future topographic and hydrodynamic monitoring will allow to fine tune our insights into the morphological response and to estimate the contribution of the different processes controlling the tidal prism in the Zwin inlet.

Contents

List of tables

List of figures

1 Project overview: aim & objectives

The Zwin is a unique nature reserve designated as Natura2000 site and situated at the border between Belgium and the Netherlands. It consists of a small tidal inlet connected to the North Sea through a tidal channel and terminates in the marsh. The Zwin forms a small tidal flood plain, exhibiting a broad range of diverse and well-organized bedforms (e.g. coastal dunes, sand banks/bars, tidal flats and other landforms) (Figure 1). The Zwin tidal inlet system is composed of two morphological units. The entrance inlet unit consists of a tidal delta where waves and tides are important constituents of the water motion and sediment transport. In contrast, tidal currents prevail over waves in the inland inlet unit. It is characterized by a main channel undergoing a sequence of bifurcation resulting in a complex pattern of meanders. The inlet is flooded twice a day and the sea floods the inland area during high tide. The water volume in the inlet is variable, depending on the tidal phase and cycle (i.e. neap and spring). Also storm surge further increases the volume of the water exchanged with the sea. The morphology of the tidal channel is controlled by hydrodynamic forcings (waves, tide), local relief and vegetation. In the past, the Zwin inlet was subject to continuous sediment deposition and siltation ranging from 3000 to 40 000 m^3/year which was mainly caused by the tidal asymmetry (Houthuys et al., 2013). As a result, areas flooding every tidal cycle were drastically reduced with some locations only inundated during spring tides. Consequently, valuable mudflats and salt marshes were disappearing, along with the native fauna and flora typical for this natural environment. In order to tackle this, large scale intervention works took place in the Zwin from August 2016 to February 2019. After the restoration work ending with the opening of the dyke, the Zwin covers a surface area > 330 ha, of which 290 ha are located on Belgian territory. It has an extension of 2.5 km along the coast ad 1.5 km inland from the dune line. These interventions thus aimed to increase the tidal prism (volume of water that enters and leaves the Zwin channel) by enabling more and faster seawater flow in and out of the channel in order to reduce the silting process. Specifically, the intention of the channel extension was to allow three times as much seawater to flow in and out by increasing the tidal prism up to 1 million m^3 (ZTAR Newsletter, 2017).

To evaluate whether the interventions achieved the desired objectives and to gain knowledge about the morphological response of the area, it is crucial to monitor the situation of the Zwin system before and after the completed works. The monitoring program covers: (i) hydro-morphodynamics, (ii) ecological, (iii) fresh-salt ground water dynamics. In this report, the results focus on the characteristics and changes of the hydro- and morphodynamics of the Zwin area over the period between the opening of the dyke (February 2019) and 1.9 year afterwards. Morphological changes from the pre-opening to the last 8 months after were presented in Montreuil et al. (2020). Topographic and hydrodynamic data obtained during the study period were processed, analysed and integrated in order to understand the post-interventions evolution of the tidal inlet.

Figure 1 – Morphological units of the tidal inlet. Unit delineated based on the 5 m contour line.

2 Topo-bathymetric data acquisition and methodology

Within the framework of this project, a large amount of data was gathered (Table 1). This data set consists of topographic and bathymetric (airborne LiDAR, Qboat, and RTK-GPS profile surveys), hydrological and sediment measurements with several sources (Coastal Division, Aqua Vision and Flanders Hydraulics Research) and times of acquisition. For their usage, an updated data timeline and a coherent storage structure of the data set was applied to assess the morphodynamics of the Zwin inlet. The presented data timeline was used to analyze and interpret the morphological evolution of the study site, taking into account the information on wave climate and tidal action (forcing factors).

2.1. Survey timeline

The morphological change of the Zwin before, immediately after and a longer time after the opening of the dyke on 04/02/2019 was investigated at a large-scale based on airborne LiDAR surveys. Also, the behaviour of the entrance inlet and inland inlet was assessed using Real-time kinematic positioning (RTK-GPS) profiles and Qboat surveys respectively.

Table 1 – Overview of the data timeline from 2019 to 2020.

2019	28/01	Lowering the old dyke
	30/01-01/02	Qboat flow and bathymetry
	04/02	Opening of the dyke
	06-07/03	Qboat flow and bathymetry
	20/04	LiDAR
	17-18/06	Qboat flow and bathymetry
	04/07	RTK-GPS cross-channel topography
	16-17/09	Qboat flow and bathymetry
	29/10	LiDAR
	11-12/12	Qboat flow and bathymetry
2020	28/2	LiDAR (post-Ciara storm on 10 Feb)
	16/03	RTK-GPS cross-channel topography
	14/4	LiDAR
	03-04/06	Qboat flow and bathymetry
	29-30/09	Qboat flow and bathymetry
	30/09	RTK-GPS cross-channel topography
	28-29/10	Qboat flow and bathymetry

Note: surveys before 2019 are reported in Montreuil et al. (2020).

2.2. Airborne LiDAR surveys

Airborne LiDAR surveys were commissioned along the entire coast by Coastal Division on 29/10/2019, 28/02/2020 (post-storm) and 10/04/2020. They are performed at low tide. For each survey, the elevation point clouds (x, y, z) were used to generate a Triangulated Irregular Network (TIN) and then converted to Digital Elevation Model (DEM) with 2 m cell size. The cell size was chosen taking into account the spacing between the surveys points (density: > 1 point/m^2). Consecutive DEMs of Difference (DoD) were calculated from the DEMs, by subtracting the elevations in each grid, on a cell-by-cell basis, in order to visualize the morphological changes after the opening of the dyke. The survey error (root-mean-square) is below 0.03 m.

2.3. RTK-GPS profiles

RTK-GPS profiles of the channel entrance were carried out by Coastal Division approximately every 6 months, while for 28/02 and 10/04/2020 additional profiles were extracted from LiDAR surveys. All the profiles extend from the coastal dunes from the west side of the Zwin to the upper-beach across the Dutch border. In general, the interval between measured points varies from less than 1 to 20 m. All profiles were interpolated with 1 m interval for further analysis. The survey error (root-mean-square) is +/- 0.05 m.

2.4. Qboat surveys

Bathymetry of the inland inlet area was surveyed by Aqua Vision using a remotely-controlled Q-Boat 1800RP system equipped with an ADCP and GPS devices. The advantage of such system is to be capable to sound the bed surface in shallow zones. Bathymetric measurements were done in January 2019 and October 2020 (Table 1 and Table 2). The reported error ranges from 2 cm in horizontal and 3 cm in vertical direction. A typical track survey is displayed in Figure 2. Regarding the post-processing, the point clouds (x ,y, z) were first converted to Lambert72 from ETRS89. Then, they were used to generate a TIN and then converted to a Qboat DEM with 0.1 m cell size (i.e. appropriate with the spacing between the surveys points). Finally, consecutive Qboat DoDs were calculated from the Qboat DEMs, by subtracting the elevations in each grid, on a cell-by-cell basis.

Table 2 – Summary of the characteristics of the Qboat surveys.

| Time	Total point clouds	Processed area (m^2)	Meteo-marine conditions
30/01-01/02/2019	157249	79899	SE, E low wind speed (<4 Bft) HW of 3.8 m TAW
06-07/03/2019	89065	49297	S, SW from medium to high wind speed (<7 Bft) Spring tide with HW of 4.4 m TAW Restriction of the survey coverage due to the occurrence of a storm
17-18/06/2019	214593	95076	NNW, NNE low wind speed Spring tide with HW of 4.5 m TAW
16-17/09/2019	215333	97814	N, NNW medium wind speed (4 Bft) Spring tide with HW around 4.6 m TAW
11-12/12/2019	249593	108512	SSW-S with calm wind speed (< 4 Bft) Spring tide with high water (HW) of 4.88 m TAW
03-04/06/2020	230454	111623	NNW with calm wind speed (< 4 Bft) Spring tide with high water (HW) of 4.50 m TAW
29-30/09/2020	260870	93850	SW with calm wind speed (2 Bft) Spring tide with high water (HW) of 4.5 m TAW
28-29/10/2020	279280	109267	SW with medium wind speed (5-6 Bft) Spring tide with high water (HW) of 4.8 m TAW
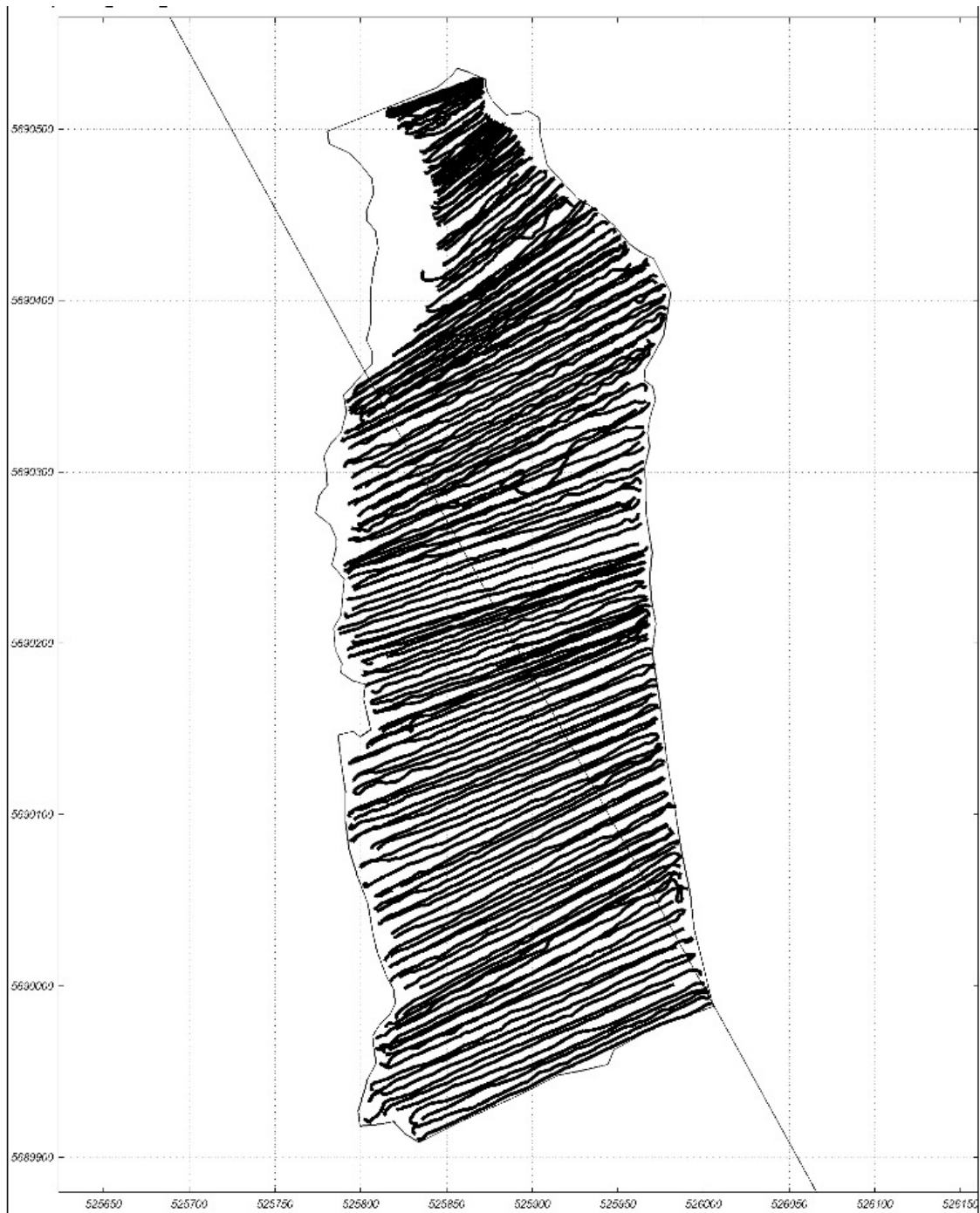
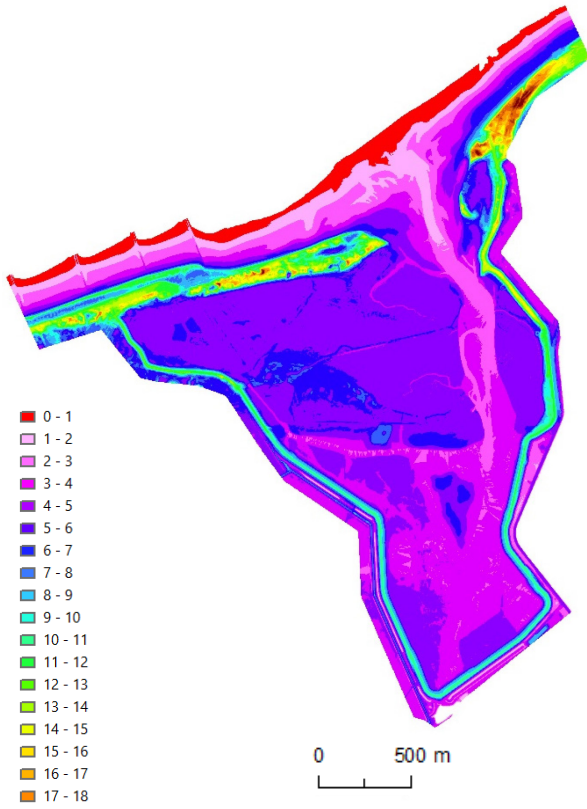Figure 2 – Example of typical tracks of a Qboat survey.

3 Morphodynamics results

3.1 Large-scale dynamics – entrance and inland inlet (LiDAR)

Based on the 20/04/2019, 29/10/2019, 28/02/2020 and 10/04/2020 LiDAR surveys, Figure 3 displays the elevation and the consecutive elevation differences of the entire Zwin inlet. The inlet is composed of a main channel of 1.3 km long from the seaward side of the entrance to the most inland side of the inlet, and it intersects the beach plain backed by the Belgian and Dutch coastal dunes. The sand flat is characterized by dynamic sandy bedforms and rimmed by tidal flats backed by salt marshes above 4.8 m TAW. In the entrance inlet unit, the main tidal channel is almost 200 m wide and oriented 130-310° (NW-SE). Its bed elevation varies from 1.4 m to 3 m TAW from seaward to landward. Noteworthily, these numbers have to be treated with caution due to the limitation of the LiDAR to penetrate water. The sandy bedforms consisting of banks and bars as well as the presence of gullies give a morphologically meandering character to the channel. The inland inlet unit is characterized by a main channel oriented 0-180° and is characterized by a width below 100 m and an average bed elevation of 2 m TAW. The channel undergoes a sequence of bifurcations resulting in a complex pattern of meandering channels and tidal flats. This thus leads to spatial variability of the width of the channel.

Significant morphological changes exceeding 2 m in height occurred at seasonal scale in the year after the opening of the dyke (20/04/2019-29/10/2019, 29/10/2019-28/02/2020), while a relative stability was observed over the two months period between 28/02/2020-10/04/2020 in the first year after the opening. After 1.4 years (06/11/2018-10/04/2020), the inland inlet unit was subject to a decrease of sediment volume of -45 296 m^3 which was equivalent to an average reduction in elevation of about 0.42 m (Table 3). At the same time, the sediment volume in the entrance inlet unit did not change so significantly. Significant morphological changes occurred in the main channel which became deeper and wider, and migrated eastward (Figure 4). Channel erosion reached its maximum exceeding 3 m depth, located on the westward edge between the entrance inlet and the inland inlet (around 600 m from the seaward entrance). Also, a spatial variability is observed in the entrance inlet with alternating accretion and erosion zones parallel to the coast as well as on the edge of the salt marsh and dune line. This footprint is typical of migration of a three dimensional pattern of sandy bedforms. In the inland inlet, erosion dominantly along the east side of the channel suggesting deepening associated with eastward migration. In contrast, the west side of the inlet is subject to a slight accretion along the edge of the salt marsh. Thus, the channel here migrates to the east.

A) 20/04/2019

E) 20/04/2019 - 29/10/2019

■	0 - 1
■	1 - 2
■	2 - 3
■	3 - 4
■	4 - 5
■	5 - 6
■	6 - 7
■	7 - 8
■	8 - 9
■	9 - 10
■	10 - 11
■	11 - 12
■	12 - 13
■	13 - 14
■	14 - 15
■	15 - 16
■	16 - 17
■	17 - 18

■	< -2
■	-2 - -1.75
■	-1.75 - -1.5
■	-1.5 - -1.25
■	-1.25 - -1
■	-1 - -0.75
■	-0.75 - -0.5
■	-0.5 - -0.25
■	-0.25 - 0
■	0 - 0.25
■	0.25 - 0.5
■	0.5 - 0.75
■	0.75 - 1
■	1 - 1.25
■	1.25 - 1.5
■	1.5 - 1.75
■	1.75 - 2
■	> 2

0   500 m
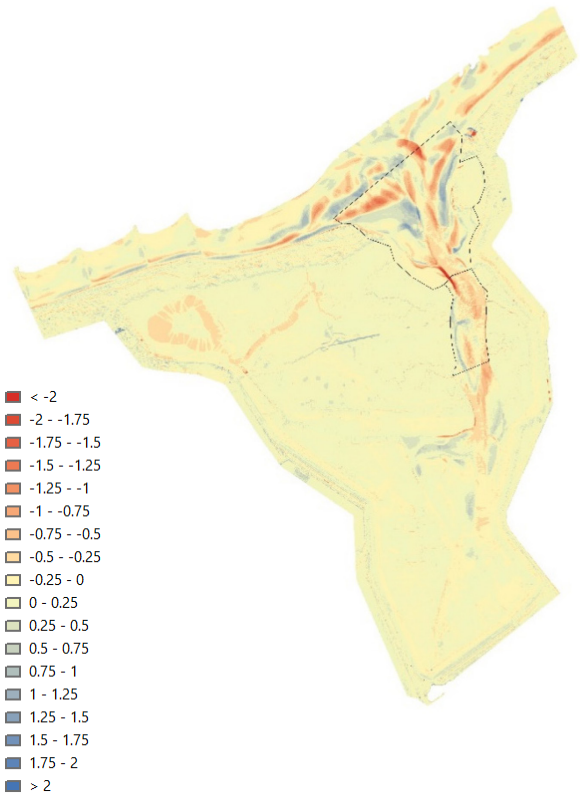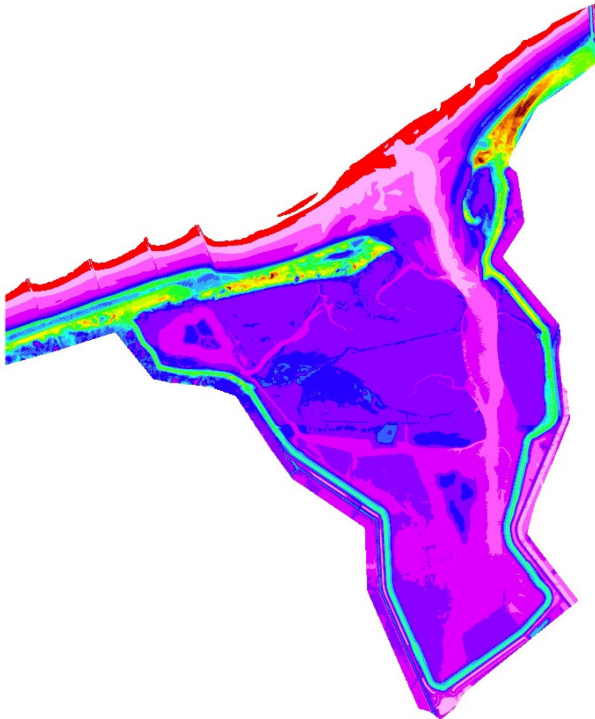
B) 29/10/2019

F) 29/10/2019 - 28/02/2020
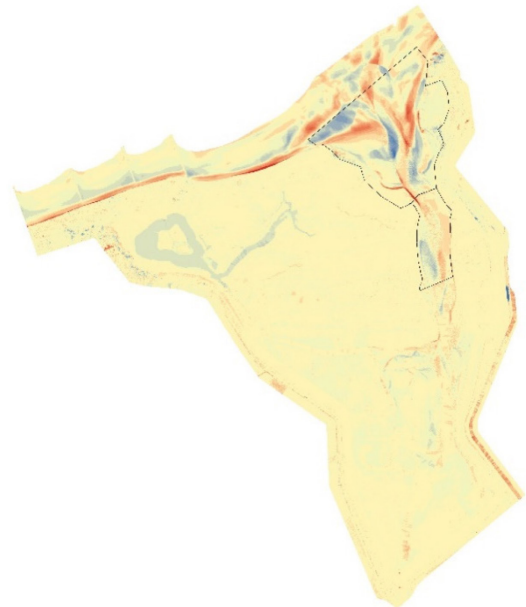
C) 28/02/2020
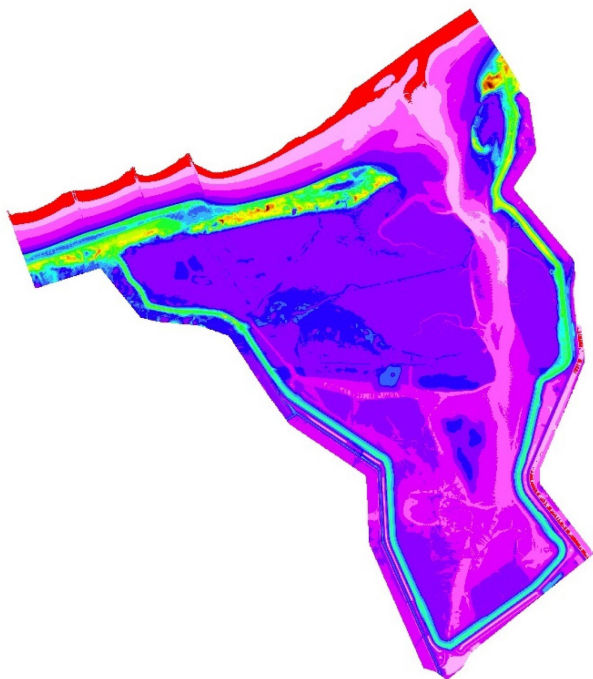
G) 28/02/2020 - 10/04/2020
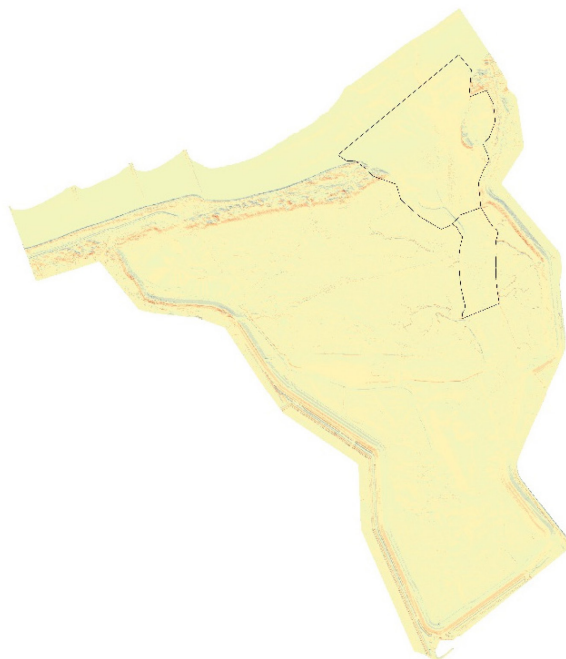
D) 10/04/2020
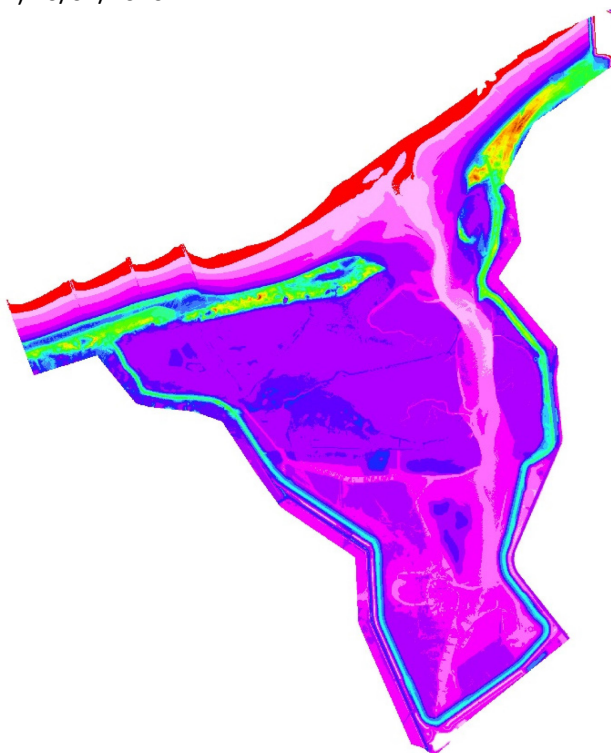
Figure 3 – LiDAR DEMs on A) 20/04/2019, B) 29/10/2019, C) 28/02/2020 and D) 10/04/2020
(i.e. from 2.5 month to 14.2 month after opening of the dyke and the consecutives DoDs (E, F, G)
Note: the grey polygons correspond to the entrance and inland inlet units.

A) 06/11/2018 - 20/04/2019

B) 06/11/2018 - 29/10/2019

■	< -2
■	-2 - -1.75
■	-1.75 - -1.5
■	-1.5 - -1.25
■	-1.25 - -1
■	-1 - -0.75
■	-0.75 - -0.5
■	-0.5 - -0.25
■	-0.25 - 0
■	0 - 0.25
■	0.25 - 0.5
■	0.5 - 0.75
■	0.75 - 1
■	1 - 1.25
■	1.25 - 1.5
■	1.5 - 1.75
■	1.75 - 2
■	> 2

0   500 m
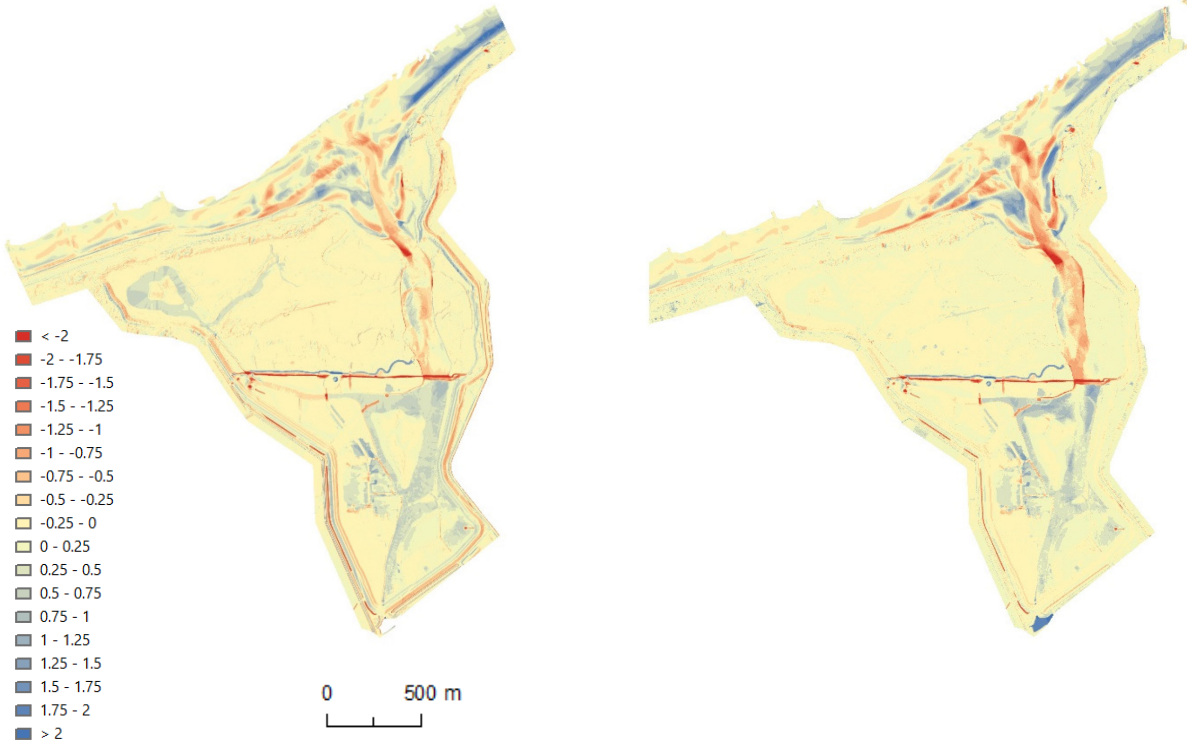
C) 06/11/2018 - 28/02/2020

D) 06/11/2018 - 10/04/2020

Figure 4 – LiDAR DoDs between the T0 survey before the opening of the dyke (06/11/2018) and the recent surveys.

Table 3 – Sediment volume in the Zwin inlet units before and after the dyke opening based on the LiDAR surveys.
Note: Area of the entrance inlet is around 446 700 m² and of 107 550 m² for the inland inlet.

	Volume above 0 m TAW (m³)	
	Entrance inlet	Inland inlet
06/11/2018 (T0 survey, before the opening of the dyke)	1749505.87	343845.56
10/04/2020 (1.4 year after the opening of the dyke)	1713172.64	298549.11
Difference	-36333.23	-45296.45
Difference normalized	-0.07 m	-0.42 m
06/11/2018	1 749 505.87	343 845.56
20/04/2019	1 747 870.05	324 809.84
Difference	-1635.82	-19035.72
Difference normalized	-0.004	-0.179
20/04/2019	1747870.05	324809.84
29/10/2019	1722883.45	306566.8666
Difference	-24986.60	-18242.97
Difference normalized	-0.043 m	-0.162 m
29/10/2019	1722883.45	306566.8666
28/02/2020	1715092.12	298167.26
Difference	-7791.33	-8399.61
Difference normalized	-0.017 m	-0.078 m
28/02/2020	1715092.12	298167.26
10/04/2020	1713172.64	298549.11
Difference	-1919.48	381.85
Difference normalized	-0.004 m	0.004 m

Note: normalized by the covered area.

3.2   Entrance inlet

Cross-channel morphology of the entrance inlet was investigated based on the RTK-GPS profiles carried out from 11/2018 (pre-opening) to 09/2020. Previous cross-shore topographic profiles are presented in the progress report after the first year (Montreuil et al., 2020). Figure 5A shows the bed elevation as a function of distance from the origin of the profile. A clear morphological change is observed in the main channel loca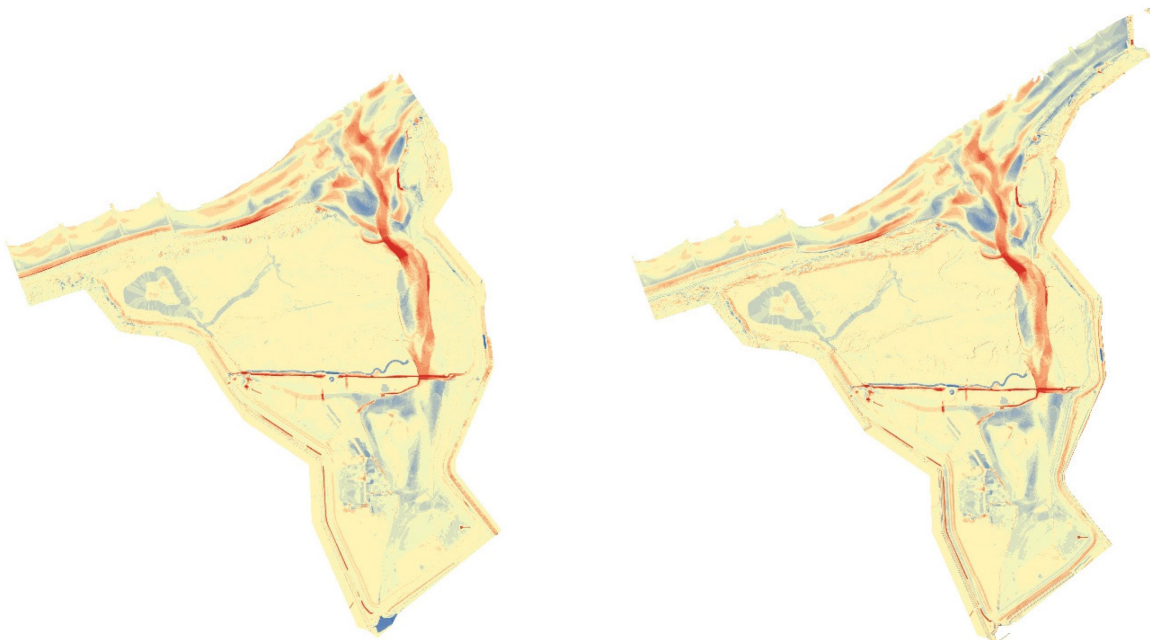ted at a distance between 260 and 350 m from the benchmark located in the west dune becoming progressively wider over time. On 30/09/2020 survey, the lowest elevation of the channel was at 1.02 m TAW, while it was at 1.71 m TAW before the opening of the dyke (07/11/2018). The channel became thus 0.69 m deeper in its centre. A large difference of elevation of 2.66 m occurred between 28/02/2020 and 04/07/2019 due to an eastward migration of the channel (Figure 5B). In addition, a sand bank exceeding 1 m high and located in the profile between 45 and 160 m present before the opening of the dyke was eroded after 04/07/2019 (Figure 5A). This is probably due to the excavation works of the tidal area carried out until the opening of the dyke.

Morphological indicators were defined and extracted from the cross-shore channel profiles (Table 5). The channel basin channel based on the spring high water reference has changed over time ranging from 994.9 m³ on 07/11/2018 to 1143.05 m³ on 10/04/2020. A comparable pattern of changes has occurred for the basin of the channel based on the neap high water reference level. Also, the width of the channel has followed a similar pattern and trend, and it was highly correlated to the basin channel.

A)

B)
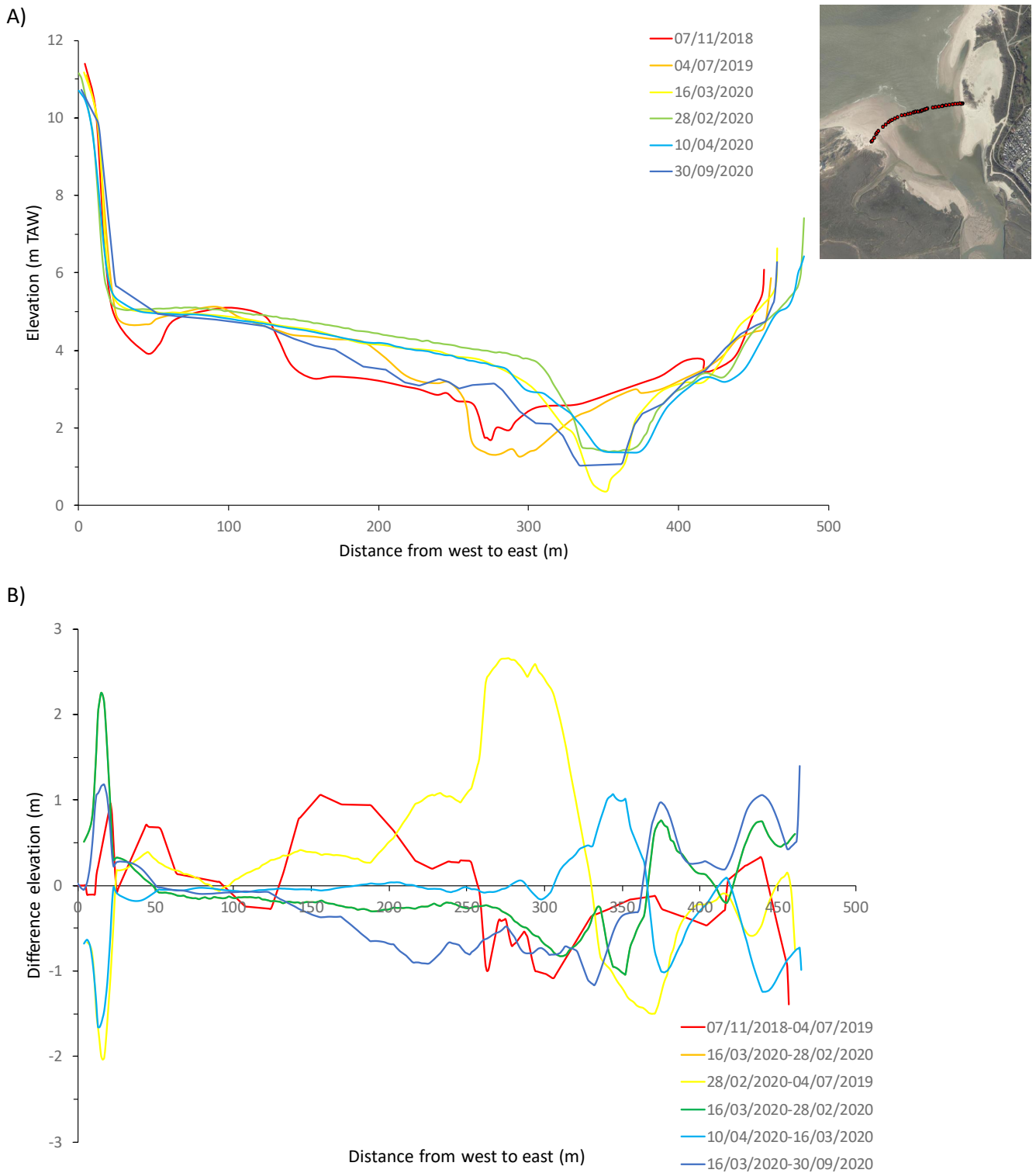
Note: profiles on 28/02/2020 and 10/04/2020 were extracted from LiDAR surveys.

Figure 5 – A) Cross-channel profiles from 11/2018 (pre-opening) to 09/2020; B) difference of consecutive surveys. Insert: location of the profile measurement. Benchmark is located in the west dune.

Table 4 – Definition of morphological indicators

Position western (eastern) edge at spring HW (neap HW)	Distance of the western (eastern) edge of the channel elevation reaching the spring high water level of 4.7 m TAW
Position western (eastern) edge at neap HW (neap HW)	Distance of the western (eastern) edge of the channel elevation reaching the spring high water level of 3.8 m TAW
Width at spring HW (neap HW)	Distance of the channel between western and eastern edge at spring HW (neap HW)
Area at spring HW (neap HW)	Surface of the channel section between western and eastern edge at spring HW (neap HW)
Volume at spring HW (neap HW)	Internal core of the channel section between western and eastern edge at spring HW (neap HW)
Avg depth spring HW (neap HW)	Average elevation in the channel section
Max depth spring HW (neap HW)	Maximum elevation in the channel section
Min depth spring HW (neap HW)	Minimum elevation in the channel section

Table 5 – Summary indicators of the cross-channel marker locations based on the RTK-GPS profiles.

	07/11/2018	04/07/2019	28/02/2020*	16/03/2020	10/04/2020*	30/09/2020
Position western edge at spring HW (m)	126.00	118.00	160.00	127.00	121.00	108.70
Position western edge at neap HW (m)	139.00	204.00	296.00	262.00	253.00	179.70
Position eastern edge at neap HW (m)	435.00	428.00	457.00	443.00	449.00	425.70
Position eastern edge at spring HW (m)	448.00	458.00	439.00	429.00	461.00	455.70
Width at spring HW (m)	322.00	340.00	279.00	302.00	340.00	347.00
Width at neap HW (m)	296.00	224.00	161.00	181.00	196.00	246.00
Area at spring HW (m^2)	518.50	517.03	285.77	364.51	454.95	548.27
Area at neap HW (m^2)	240.56	270.40	243.56	264.00	214.63	291.52
Volume at spring HW (m^3)	994.90	1080.98	1025.53	1054.89	1143.05	1082.63
Volume at neap HW (m^3)	884.24	580.80	368.24	423.81	530.17	643.28
Avg depth spring HW (m TAW)	3.09	3.18	3.46	3.34	3.37	3.12
Max depth spring HW (m TAW)	4.77	4.73	4.71	4.70	4.70	4.70
Min depth spring HW (m TAW)	1.71	1.25	1.39	0.37	1.36	1.02
Avg depth neap HW (m TAW)	3.84	2.60	2.58	2.55	2.72	2.64
Max depth neap HW (m TAW)	2.99	3.81	3.80	3.81	3.83	3.81
Min depth neap HW (m TAW)	1.71	1.25	1.39	0.37	1.36	1.02

* profiles on 28/02/2020 and 10/04/2020 were extracted from LiDAR surveys.

3.3   Inland inlet

Figure 6 presents the bathymetric DEMs from the Qboat surveys in the inland inlet part from 07/2017 to 10/2020. A clear development of a main channel is visible in the inland inlet from 03/2019 (1 month after the opening) and it has gradually become deeper over the following 1.9 year period. In 10/2020, the north of the survey area is characterized by a wider and deeper channel compared to the pre-opening surveys, with the bed now below 0 m TAW. The channel is clearly asymmetric: the east side of the channel is significantly deeper than the west side. Also, a progressive eastward migration of the channel is observed associated with its deepening (in 10/2020 the deepest part is around 1 m TAW). In addition, the inland inlet is characterized by a large tidal bank with its crest up to 4 m TAW on the west side as well as smaller features such as bars and megaripples along the channel. A large sand bar is enclosed by the main channel and its small meander.
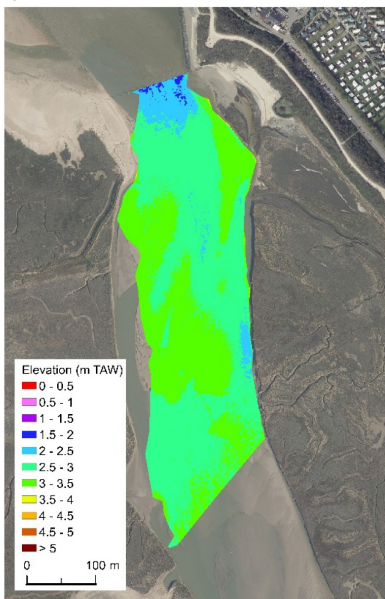
A) 10-11-12/07/2017   B) 18-19/12/2017   C) 12-13/04/2018
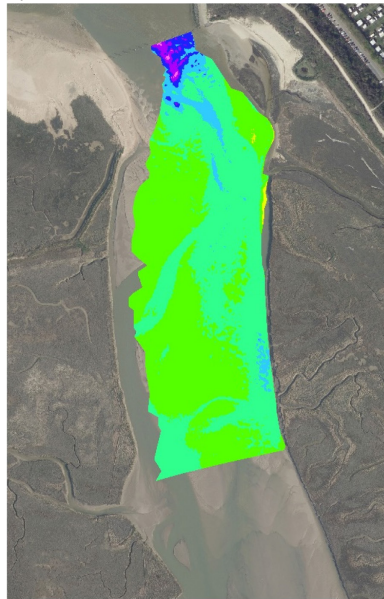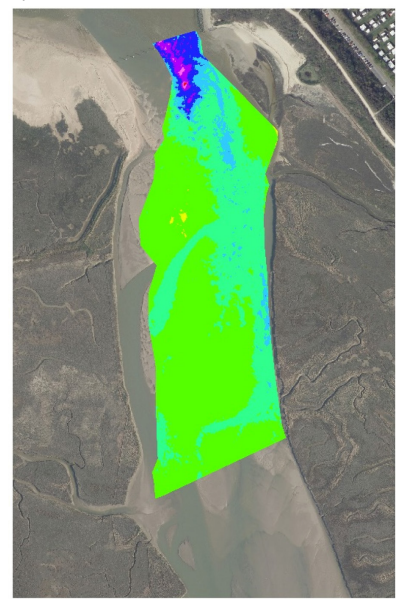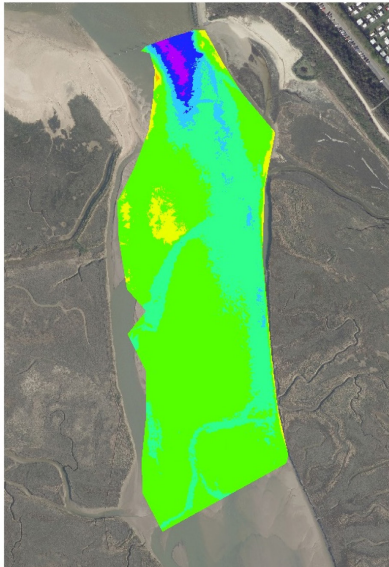
D) 10-16/07/2018   E) 23-24/10/2018   F) 31/01-01/02/2019
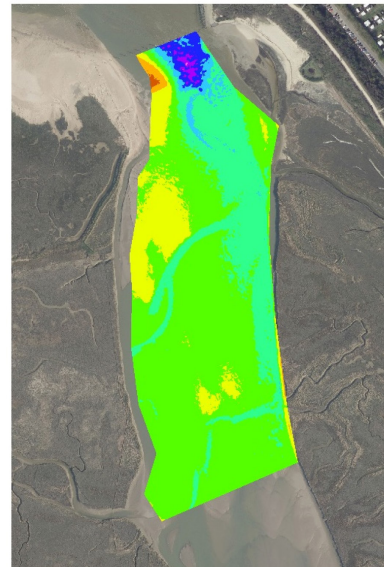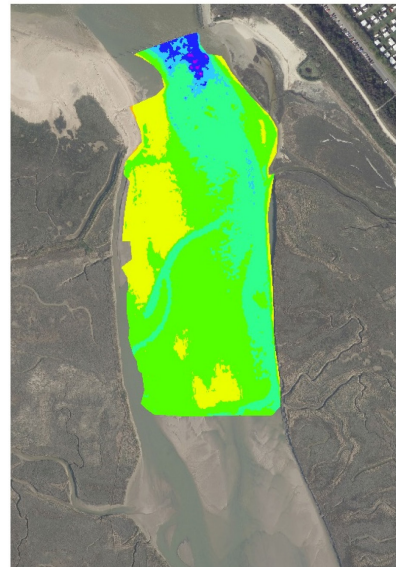
G) 06/03/2019
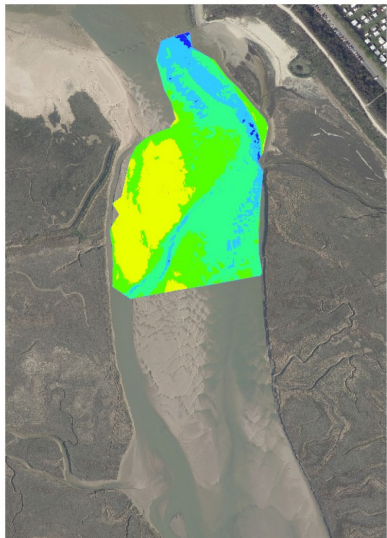
H)17-18/06/2019
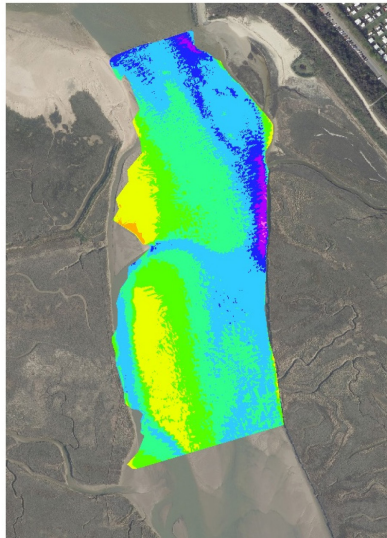
I)16-17/09/2019
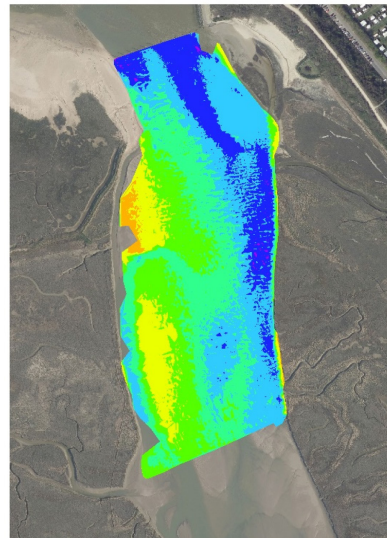
J) 11-12/12/2019
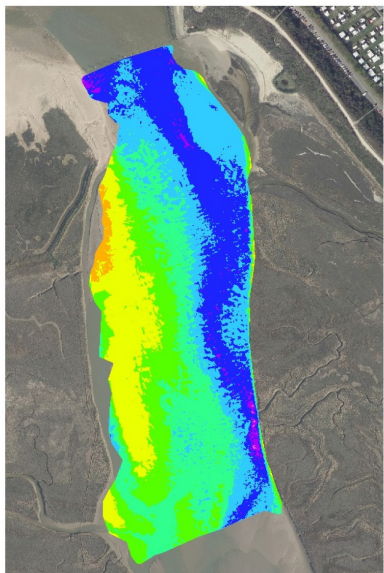
K) 03-04/06/2020
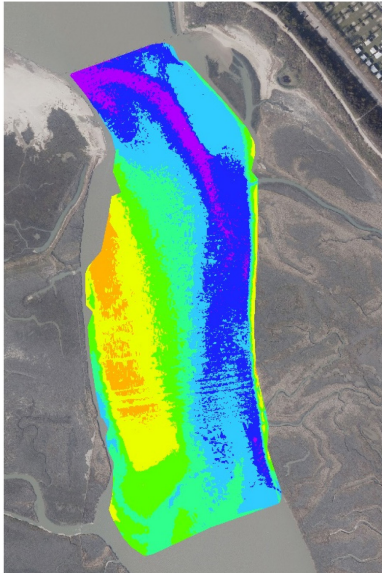
L) 29-30/09/2020
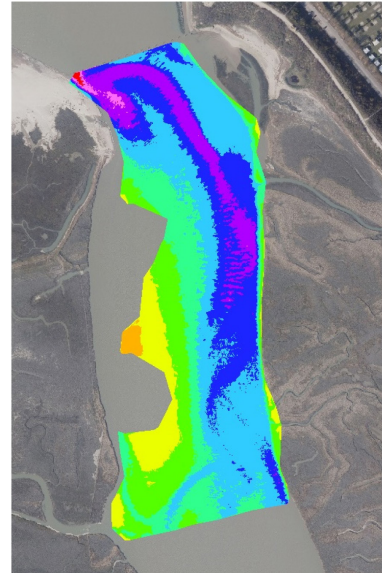
M) 28-29/10/2020
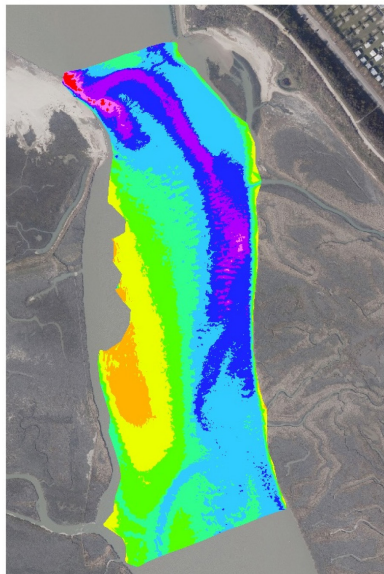
Note: coverage of the surveys mainly varied depending on the
meteorological and local topographic conditions during the data acquisition.

Figure 6 – Qboat DEMs of the inland inlet of the Zwin.

A) 07/2017 – 12/2017
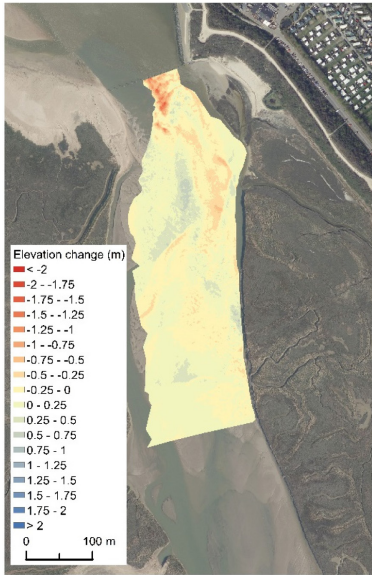
B) 12/2017 – 04/2018

C) 04/2018 – 07/2018

D) 07/2018 – 10/2018

E) 10/2018 – 01/2019

H) 01/2019 – 03/2019
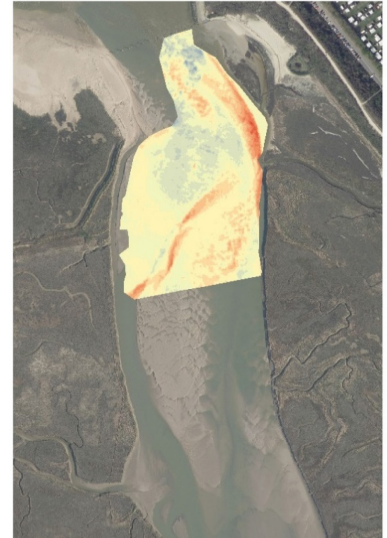
G) 03/2019 – 06/2019
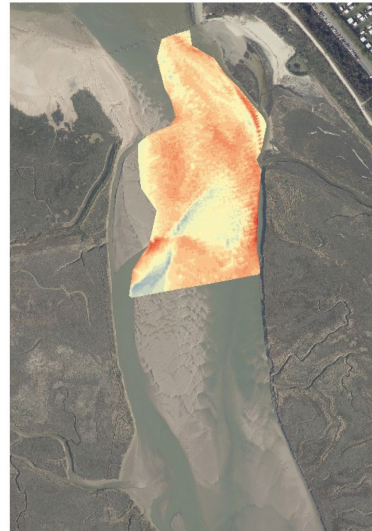
H) 06/2019 – 09/2019

I) 09/2019 – 12/2019

Elevation change (m)

< -2
-2 - -1.75
-1.75 - -1.5
-1.5 - -1.25
-1.25 - -1
-1 - -0.75
-0.75 - -0.5
-0.5 - -0.25
-0.25 - 0
0 - 0.25
0.25 - 0.5
0.5 - 0.75
0.75 - 1
1 - 1.25
1.25 - 1.5
1.5 - 1.75
1.75 - 2
> 2

0   100 m

J) 12/2019 – 06/2020   K) 06/2020 – 09/2020   J) 09/2020 – 10/2020
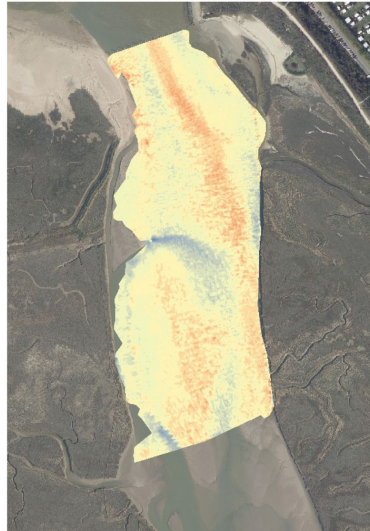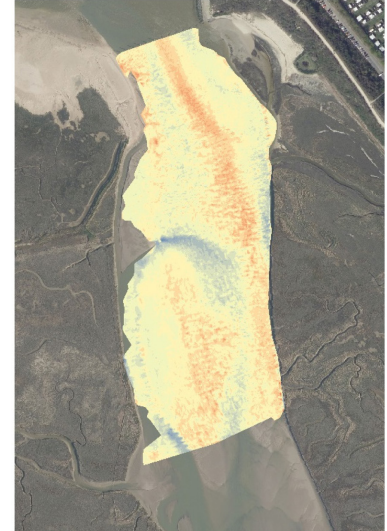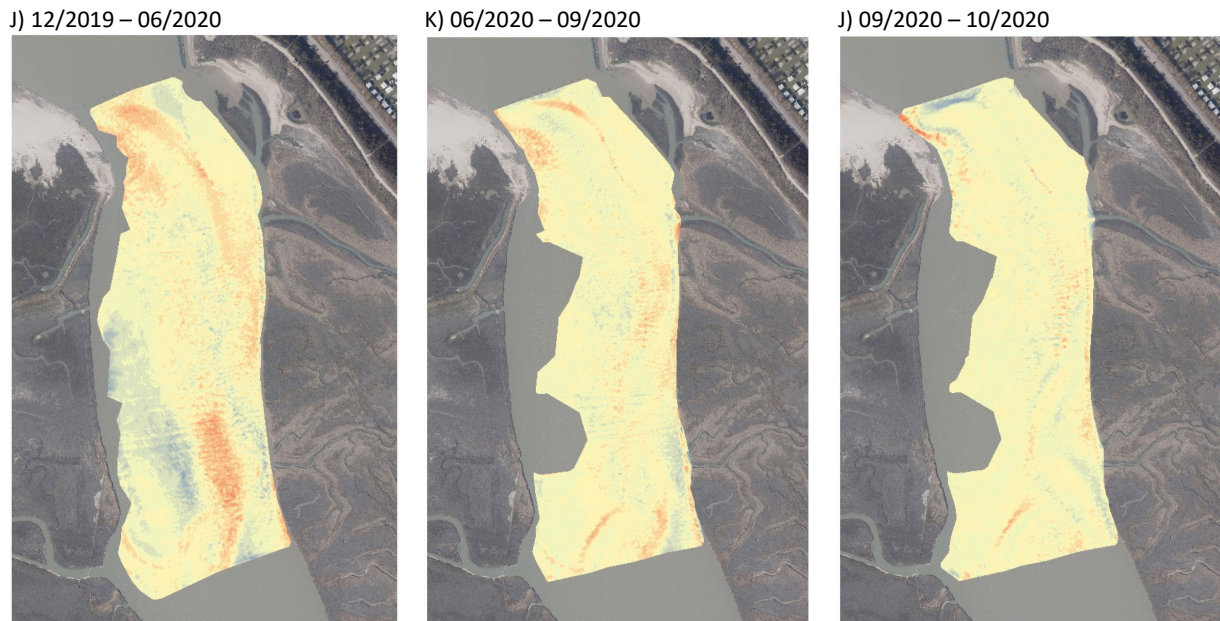
Figure 7 – Consecutive Qboat DoDs of the inland of the Zwin.

The consecutive DoDs show elevation change between surveys (Figure 7). A high spatial and temporal variability of morphological change in the inland inlet is observed. Generally, erosion occurs in the main channel and along its banks. Also, erosion is observed in the seaward part of the inland inlet except between 09-10/2020 when eroded sand from the sand bank was transported to the middle of the channel. In contrast, the large tidal bank on the west side generally experiences positive elevation change, and thus the sand volume increased. Interestingly, large morphological changes occurred from 03/2019 to 06/2019 when energetic wave conditions were recorded (Montreuil et al., 2020). The comparison between the pre- and post-opening dyke bathymetric surveys clearly shows two opposite morphodynamics trends occurring in the inland inlet namely a sediment gain westward, while erosion dominates in the east and middle of the survey area (Figure 8). Over the 1.9 year period (01/2019-10/2020), the inland inlet has become deeper with an average of nearly 0.6 m, which corresponds to a decrease of elevation of 0.032 m/year (Table 6). The deepest part of the channel was 0 m TAW in 10/2020, while it was above 1 m TAW before the opening of the dyke.
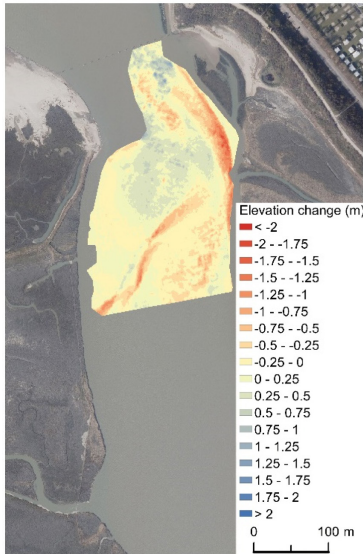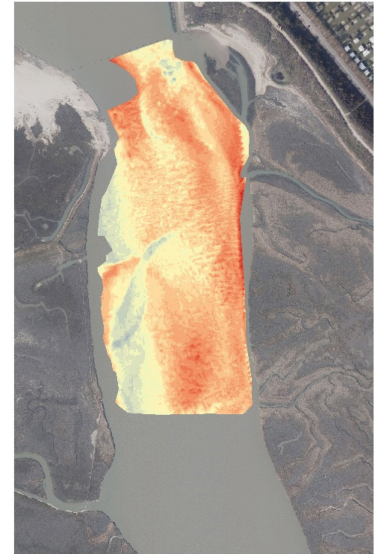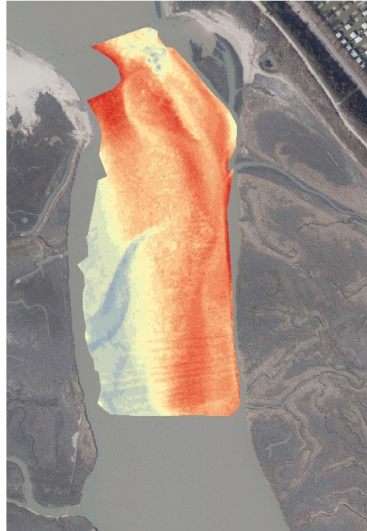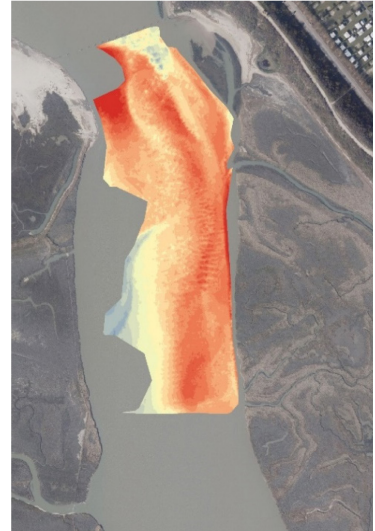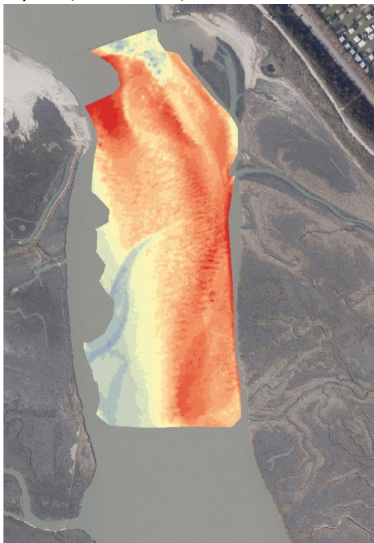
Figure 8 – Qboat DoDs of the inland of the Zwin based on a reference survey on 30/01/2019 (pre-opening dyke survey).

Table 6 – Statistic summary of the Qboat DoDs.

DoD consecutive	Difference of elevation (m)			
Survey	Mean	Max	Min	SD
07/2017-12/2017	0.010	0.823	-1.799	0.208
12/2017-04/2018	0.037	1.339	-2.072	0.181
04/2018 - 07/2018	0.033	1.559	-1.035	0.123
07/2018-10/2018	0.110	1.304	-0.919	0.134
10/2018-01/2019	0.016	1.894	-1.116	0.169
01/2019-03/2019	-0.043	1.501	-2.059	0.347
03/2019-06/2019	-0.425	1.262	-2.434	0.412
06/2019-09/2019	-0.040	1.807	-1.488	0.304
09/2019-12/2020	-0.053	1.526	-1.991	0.332
12/2019-06/2020	-0.006	1.515	-1.708	0.305
06/2020-09/2020	-0.017	1.774	-1.343	0.196
09/2020-10/2020	0.018	1.542	-1.695	0.178
DoD Ref Jan 2019				
01/2019-03/2019	-0.043	1.501	-2.059	0.347
01/2019-06/2019	-0.461	0.984	-3.064	0.465
01/2019-09/2019	-0.487	1.103	-2.415	0.485
01/2019-12/2019	-0.534	1.144	-2.396	0.574
01/2019-06/2020	-0.546	1.376	-2.650	0.721
01/2019-09/2020	-0.759	1.403	-2.835	0.631
01/2019-09/2020	-0.593	1.364	-2.960	0.724

Results of the four extracted profiles from 07/2017 to 10/2020 are shown in Figure 9. Profile 1 located at the seaward side of the inland inlet indicates that the bed elevation of the channel after the opening has progressively become deeper. The lowest elevation just before the opening of the dyke was of 1.21 m TAW, while it was below 0 m TAW in 10/2020. In addition, the channel is more than two times wider nowadays than before the opening (based on the 2 m contour line). Profile 2, 3 and 4 also indicate a similar trend with the channel becoming deeper and wider in the middle and southward side of the inland inlet over time. Another observation is the development of sand banks and their dynamics, which likely influence the topographic evolution of the channel. Decametre mega-ripples, also called submerged dunes, are observed in the channel along the four profiles. These mega-ripples indicate an active sediment transport driven by tidal currents.
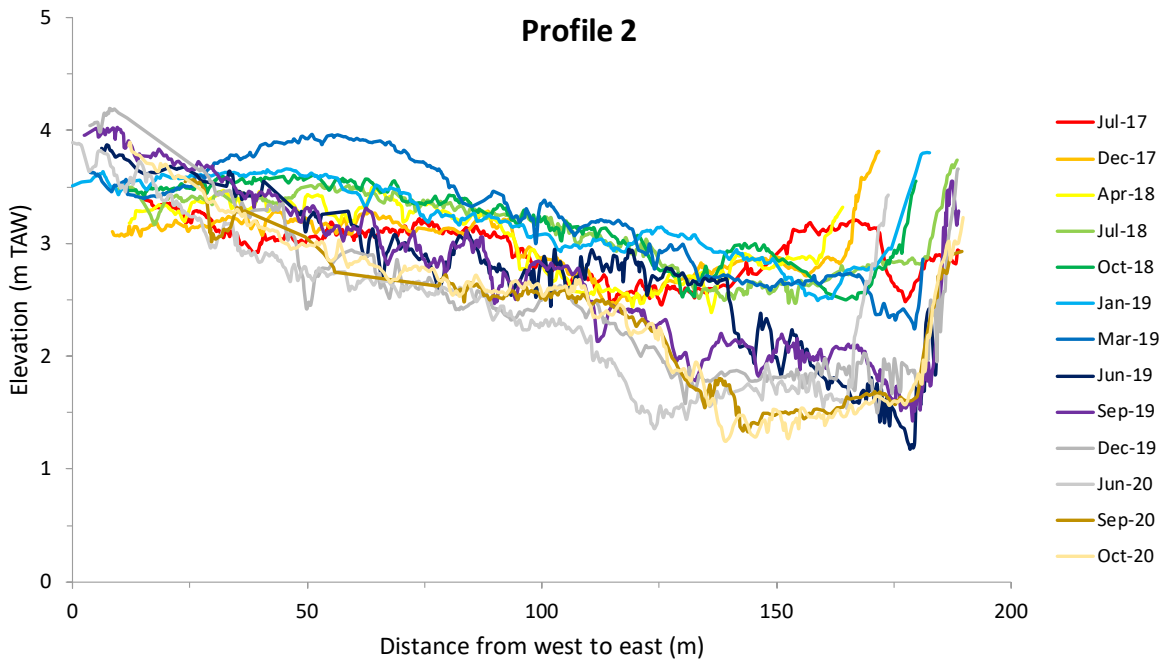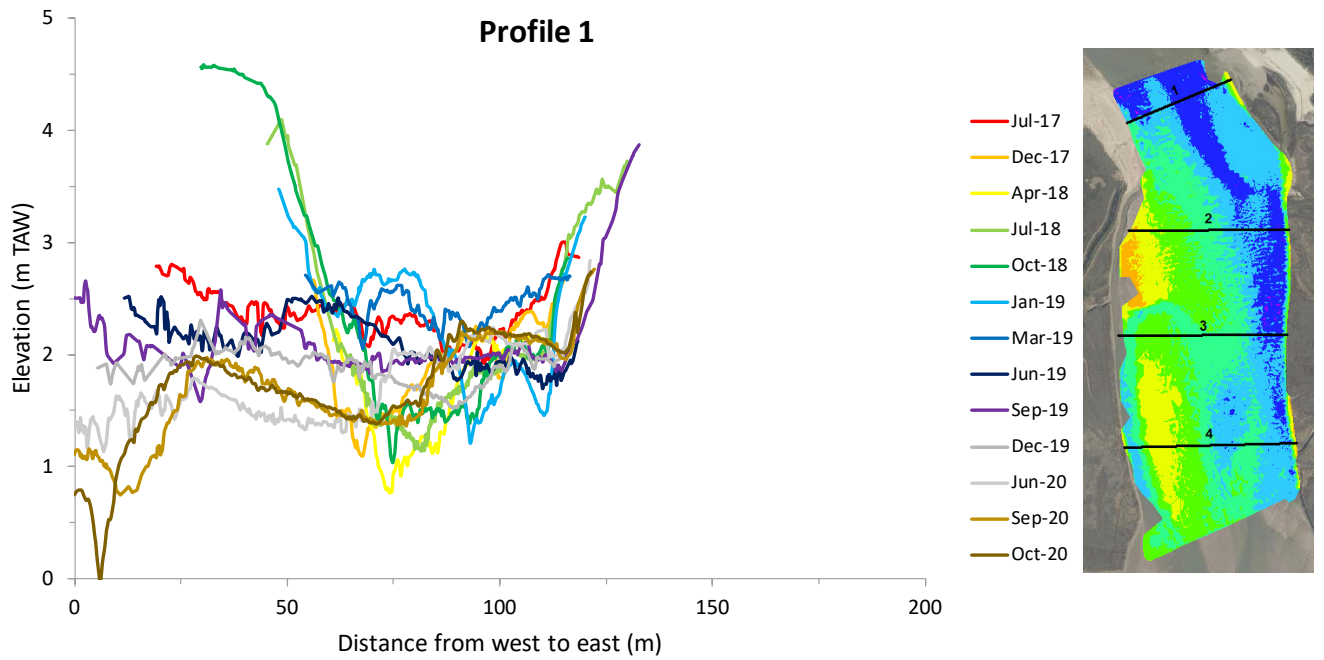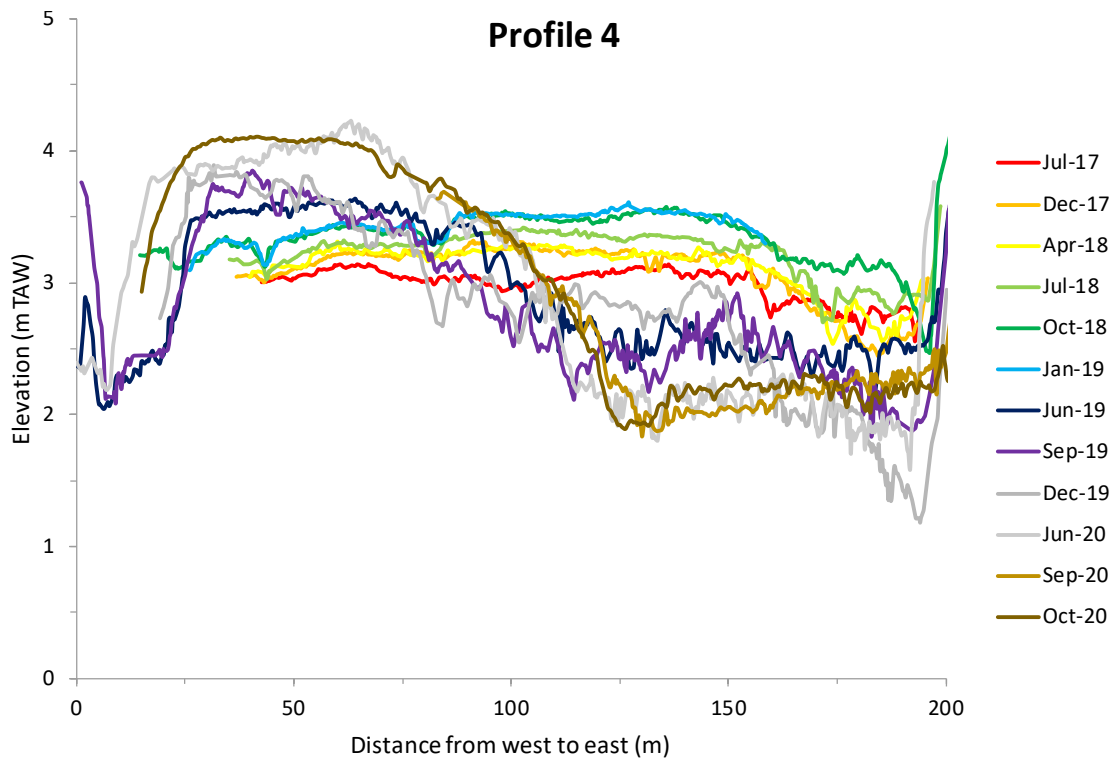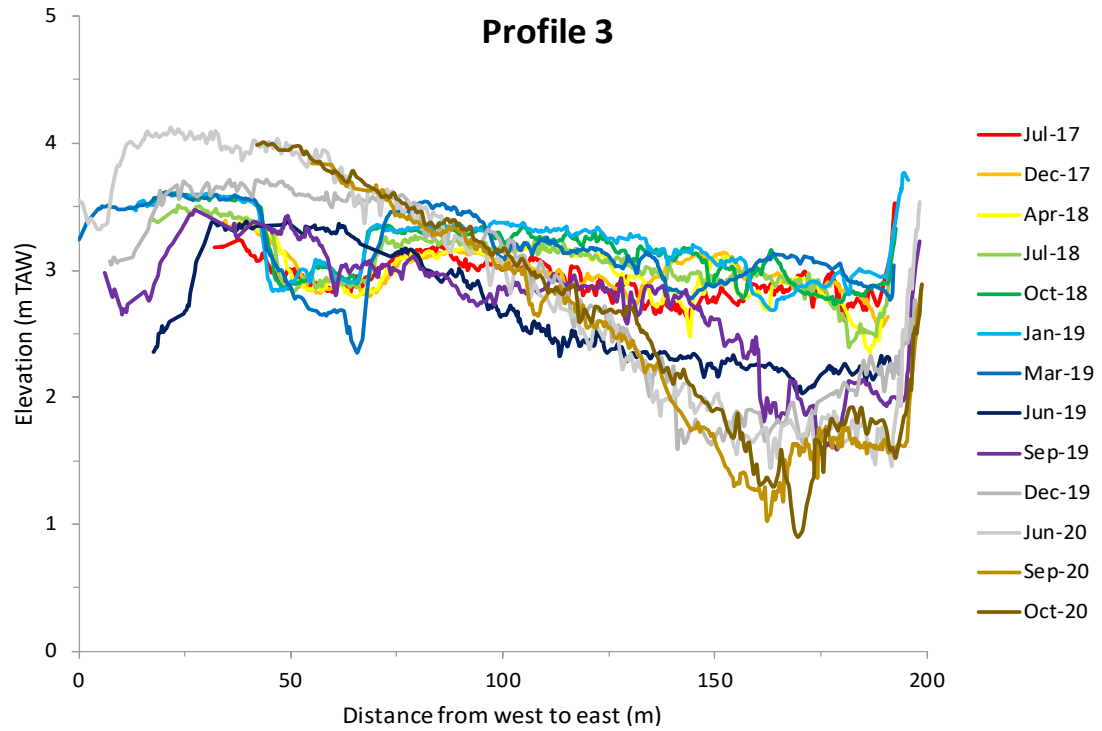
Figure 9 – Extracted profiles from the Qboat DoDs.

4 Forcing factors

4.1 Marine conditions

Water level records with 5 minutes interval were acquired from the wave buoy at Scheur located around 7 km from the study site (Table 7). Additionally, the average wave height, 10 % wave height (i.e. the wave height above which the top 10 % of the highest waves occur), period, current velocity and current direction were measured continuously at Zwin buoy located 2 km offshore from the study site

Table 7 – Description of the continuous measurement stations collected from meetnet Vlaamse Banken.

Parameter	Location	Temporal resolution
Wave: -Average wave height (m) -Average wave period (s) -Direction (°)	Scheur in 2018 7 km from the study site Depth of - 9.7 m TAW Wave direction not measured there Zwin from 2019 2 km from the study site Depth of - 8 m TAW	30 min
Water level (m TAW)	Scheur 7 km from the study site Depth of - 9.7 m TAW	5 min

In total, 3 storm surges were recorded at the coast from 11/2018 with two events in 2019 and one in 2020 (Figure 10 and Table 8). The maximum water level during these storm surges ranged from 5.39 m to 5.61 m TAW. The highest water level occurred on 10-11/02/2020 (Ciara storm) when a surge of 0.91 m was recorded. The average wave height and 10 % highest wave height were 1.85 m and 2.36 m respectively during this event.

Table 8 – Description of the past storm surges over the study period from 11/2018.

Storm surge	Maximum water level (m TAW)	Surge (m)	Average wave height (m)	Wave direction (°)	Wave period (s)
08/01/2019 (peak at 14:25)	5.39	1.09	2.68 [2.96]		5.69
30/09/2019 (peak at 01:00)	5.51	0.41	2.08 [2.65]	309	4.86
10-11/02/2020 (peak on 10/02 at 13:10)	5.61	0.91	1.85 [2.36]	302	4.95
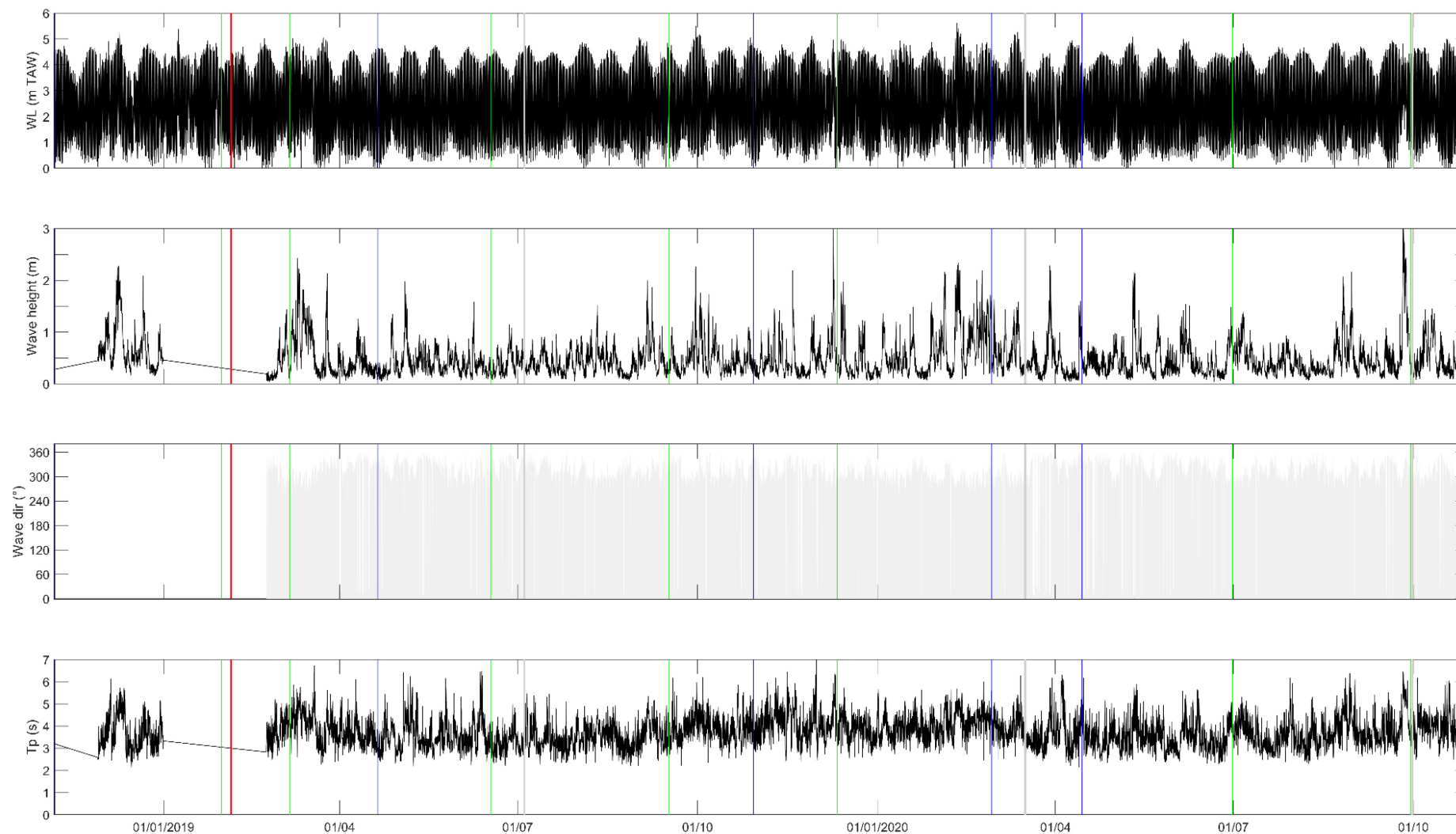
Figure 10 – Time series of water level at Scheur, average wave height, wave direction and wave period at at Scheur in 2018 and at Zwin from 02/2019.
Blue vertical lines correspond to the LiDAR surveys, green lines to the Qboat surveys, grey lines to the RTK-GPS profile surveys and red line to the opening of the dyke.

Forcing conditions were analysed to get insights about the hydrodynamics driven the morphodynamics of the Zwin inlet before and after the opening of the dyke. Figure 11 presents wave height and direction statistics for the periods between Qboat surveys starting from 09/2019. Previous periods are presented in the first progress report (Montreuil et al., 2020). Generally, the waves are coming from the sector 290-340° (WNW-NNW) and the average wave height is normally below 0.5 m. The dominant wave direction is 330-320° (NW) which is aligned with the entrance of the Zwin channel. Under energetic conditions, high waves are thus likely to enter in the inlet and then to influence the local morphology. Wave regimes from 16/09/2019-29/09/2020 was relatively similar with the highest wave ranging from 2.34 m between 11/12/2019-03/06/2020 to 3.41 between 06/2020-09/2020. Wave heights between 29/09-28/10/2020, were however lower (maximum 1.41 m) and also the spreading of waves exceeding 1 m high was limited. This short monitoring period was thus characterized by calm wave energy.
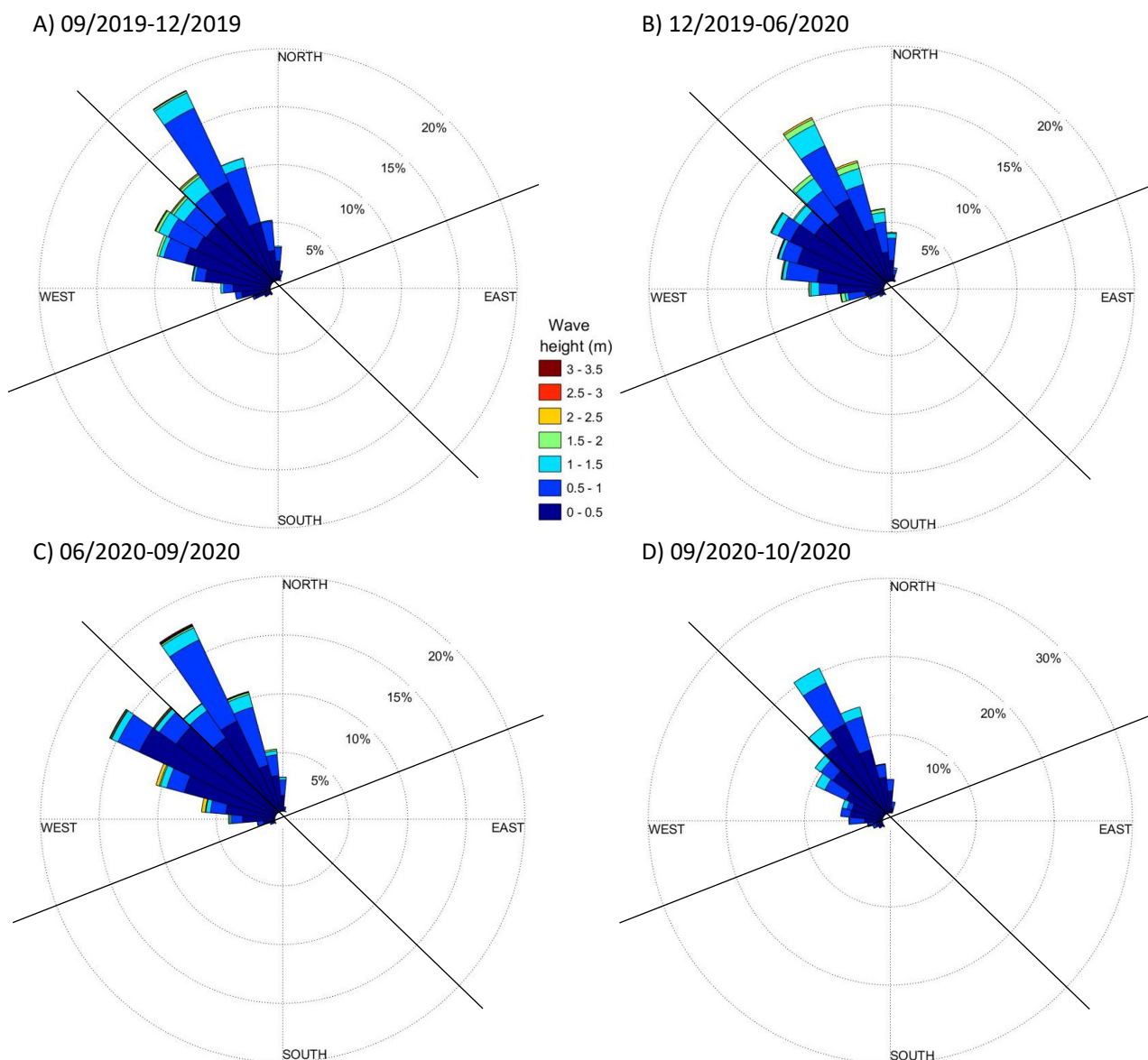
Figure 11 – Average wave distributions per Qboat survey periods measured from the Zwin buoy.
The coastline and the Zwin entrance channel are oriented WSW-ENE (70-250°) and NW-SE (130-310°) respectively.

4.2 Ad-hoc measurement campaign in the inland inlet channel

One of the main processes characterizing the morphodynamics of the Zwin system is the water storage, the volume of water which enters and leaves the marsh through the channel at each tide, also called tidal prism. In tidal inlets, there is a strong relationship between the dynamics of the water storage and the morphological state of the access channel (i.e. erosion, accretion, stability).

The processes and interrelations between hydro- and morphodynamics control the Zwin inlet evolution. Therefore, it is crucial to understand the physical processes driving the morphological changes under typical and storm conditions. This is possible by carrying out in-situ measurements. The first in-situ ad-hoc measurements campaign was carried out by FHR at the entrance of the Zwin inlet on 4-5/07/2019 under calm conditions. Results were reported in the first report (Montreuil et al., 2020). A second campaign took place in the inland inlet (nature reserve) on 5-16/12/2019 when the conditions were energetic. The objectives of the December 2019 ad-hoc measurement campaign were to determine the hydrodynamics during energetic conditions. Also, the characteristics of the water discharge were estimated in the inland inlet and compared to the Qboat discharge survey by Aqua Vision on 11-12/12/2019 (Aqua Vision, 2019).

4.2.1 Period and conditions of the December 2019 measurements

Meteo- and marine conditions were recorded at the continuous offshore stations at Scheur and Zwin located around 7 km and 2 km respectively from the study area. The ad-hoc measurements were carried out from 5/12 at 16:00 MET (i.e. all sensors deployed at 15:00) to 16/12 at 9:00 (all sensors retrieved at 9:30) during a neap-spring tide period. The total duration of the measurement campaign was of 10 days and 17 hours covering 21 flood and ebb phases.

Figure 12 and Table 9 present the recorded meteo-marine parameters at Scheur and Zwin buoy (Source: Meetnet Vlaamse Banken) during the ad-hoc measurement campaign. Energetic weather conditions prevailed with an average wind of 10.64 m/s coming from SW-WNW. A maximum wind speed of 19.6 m/s occurred on 9/12 at 12:00 which led to high waves reaching up to 3.06 m. In general, the average wave height recorded by the Zwin buoy station was 0.75 m (average Hs 0.95 m). The highest water level was 5 m TAW at the Scheur station which took place on 13/12 at 12:00. There, the current velocity ranged from 0.05 to 1.52 m/s with an average of 0.54 m/s during the entire duration of the measurement campaign.
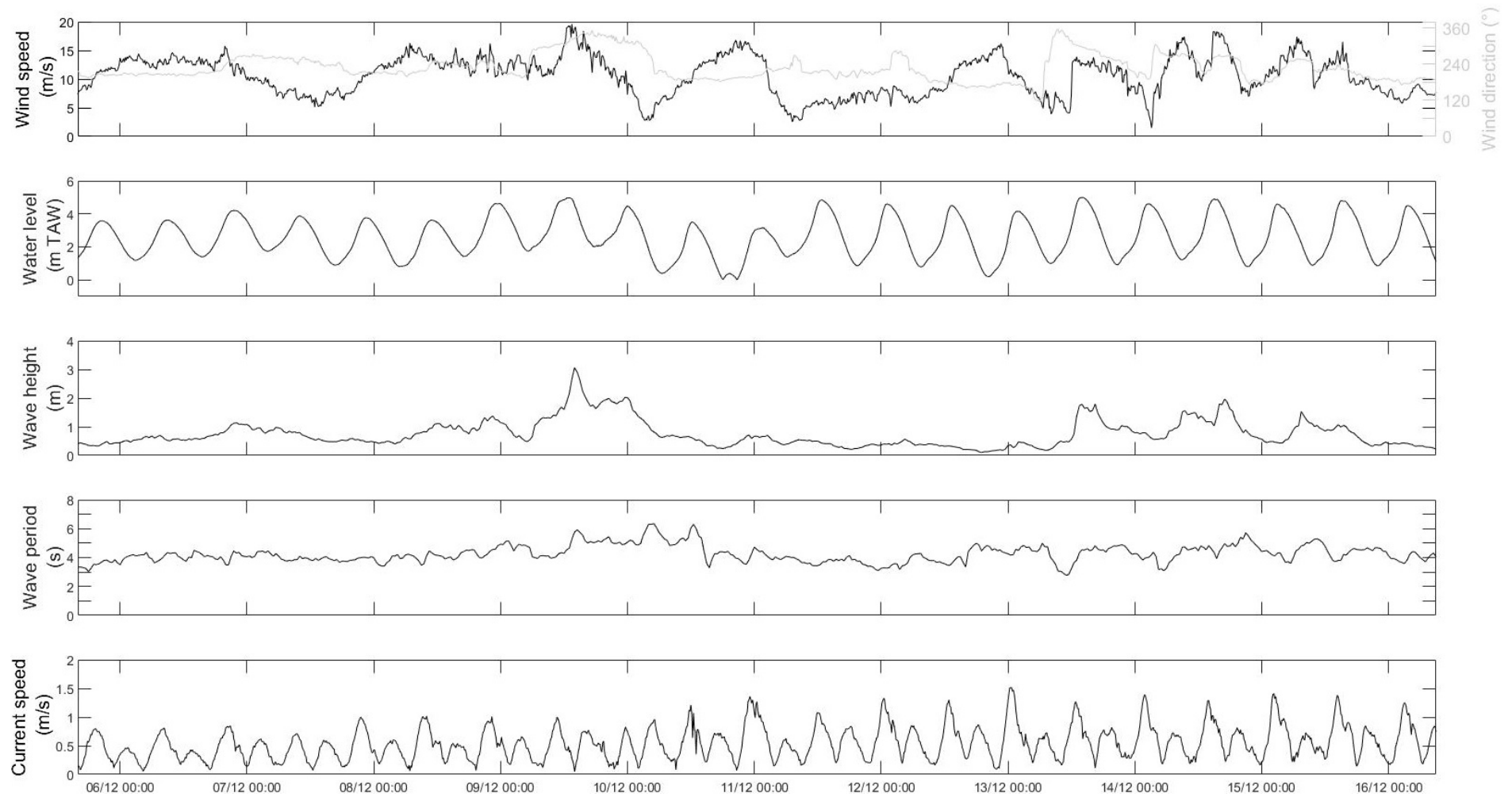
Figure 12 – Summary of meteo-marine conditions recorded at the stations during the December 2019 ad-hoc measurement campaign.

Table 9 – Summary of meteo-marine conditions recorded at the stations during the December 2019 ad-hoc measurement campaign.

Parameter	Location	Condition
Wind speed	Scheur 7 km from the study site measuring at 10 m high	Avg: 10.64 m/s Max: 19.6 m/s
Wind direction	Scheur 7 km from the study site	Avg: 229° Max: 355°
Water level	Scheur 7 km from the study site; Depth of - 9.7 m TAW	Avg: 2.58 m TAW Highest high tide: 5 m TAW
Wave parameters	Zwin (ZHG) 2 km from the study site; Depth of - 8 m TAW	Avg H: 0.75 m Max H: 3.06 m
Currents	Scheur ADCP cell 3 from 3.75 m to 6.25 m below the water surface	Avg: 0.54 m/s Max: 1.52 m/s

4.2.2   Locations of the measurements

The location of the deployed 3 sensors and the measured cross-channel topographic profile are presented in Figure 13 and Table 10. The Aquadopps were dug into the sand using a krinner mounting screw or a drill mounting construction (Figure 14). To secure the sensors, they were attached with a rope to the permanent poles in the nature reserve of the Zwin area. The head of the three Aquadopps were c. 0.1 m above the bed.

Table 10 – Description of the locations and deployments of the sensor frames.

Sensor	Coordinates (Lambert72)	Elevation (m TAW)	Description of the location
Aquadopp A (Aqd A)	80464.352E 228835.368N	2.15	West side of the channel
Aquadopp B (Aqd B)	80508.758E 228844.382N	2.47	Centre of the channel
Aquadopp C (Aqd C)	80534.665E 228835.368N	2.01	East side of the channel
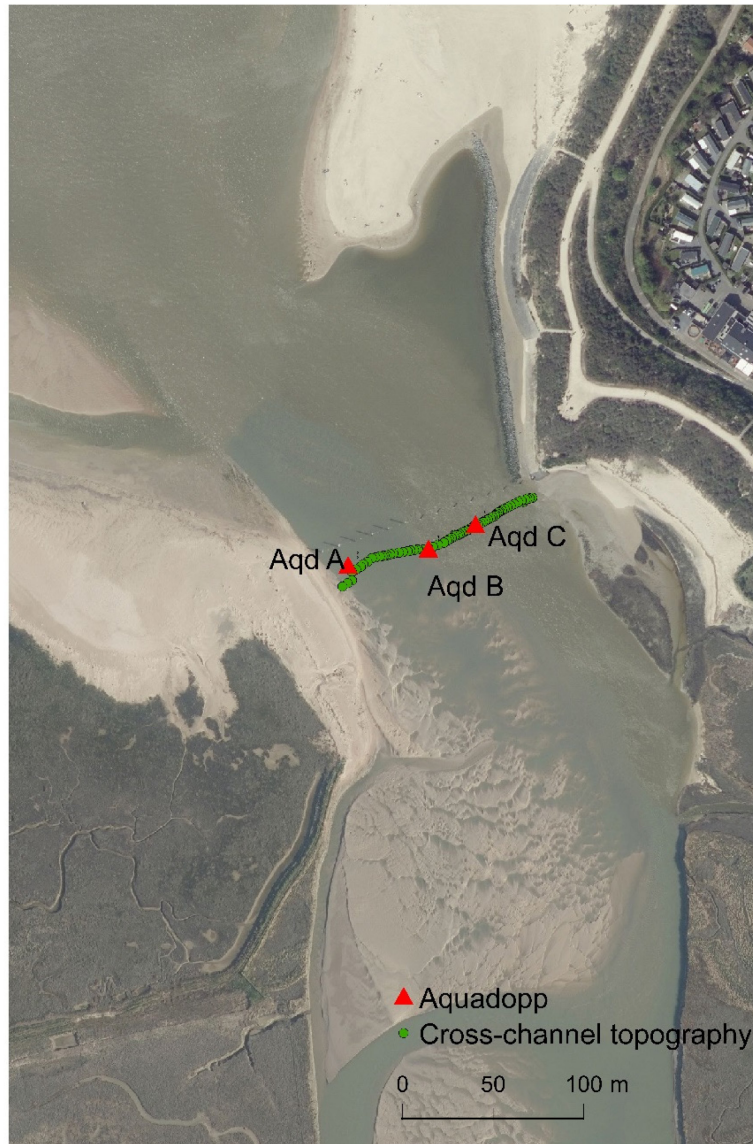
Figure 13 – Location of the ad-hoc measurement with cross-shore profile (green dots) and Aquadopp sensors (red triangles).

Figure 14 – Photographs taken during the deployment of the Aquadopp sensors.

4.2.3 Conventions

Table 11 summarizes the conventions used for the measurements.

Table 11 – Conventions used.

Item	Convention
Coordinates	Lambert72
Elevation	m TAW
Time	Winter time, MET (UTC+1h)
Current velocity	m/s
Current direction	Degree relative to North (°)
Wave height	M
Water level	m TAW
Total water discharge (cross-section of the channel of 1 m wide)	m^3

4.2.4 Methodology

A. Currents

Description: Three Aquadopp profilers were used to measure the current velocity and direction in multiple layers through the water column. They measured flow velocities in the three directions eastward, northward and vertical (Table 12).

Principle of operation: The Aquadopp sensor measures flow in a set of cells along three acoustic beams pointing in different directions to obtain the current profiles using the acoustic Doppler effect technology (i.e. based on difference of transmitting a short pulse of sound and receiving its echo). The blanking, the distance between the instrument transducers and the closest control volume (layer) within which no measurement takes place was around 0.2 m. All the Aquadopp sensors were set-up in Normal mode.

Heading, Pitch and Roll: The three sensors were stable with generally limited heading, pitch and roll motions of less than 5° which is acceptable.

Related software and output files: The data were processed using Storm software (Nortek). They contain velocity and direction of currents in the two horizontal and vertical directions for each cell through the water column, as well as, tilt, pressure, sea temperature and other sensor characteristics. Time reference of the data is in winter time.

B. Waves

Description: Wave height, period and direction were additionally measured by Aquadopp B.

Principle of operation: The sensor is set-up in wave bursts which is sequential mode (i.e. the system first collects a current profile, then wave data for a period of time determined by the number of samples and the sampling rate). Wave measurements are also based on the Doppler effect principle.

Related software and output files: The data retrieved contain information about wave parameters. Data processing was carried out with Storm software. Data are measured time is in winter time. The offsets of the mounting height above the bed was assumed to be 0.1 m. Table 10 summarizes the ad-hoc hydrodynamic measurement settings.

Table 12 – List of the ad-hoc hydrodynamic measurement settings.
Definition of the setting parameter described in the text.

Sensor	Measurement	Profile interval (s)	Average interval of measurement period (s)	Cell size (m)	Blanking distance (m)	Sampling frequency
Aqd A	Current	120	60	0.1	0.21	
	Current	120	60	0.1	0.20	
Aqd B	Wave	3600 with 1200 samples		0.5	0.20	2Hz
Aqd C	Current	60	60	0.1	0.21	

C. Cross-channel topography

A cross-channel topographic profile was carried out along the monitoring profile on 5/12/2019 using a Real Time Kinematic- GPS system (GCX3 Sokkia model). The error is about 3 cm in vertical (Claeys and Vereecken, 2019).

D. Estimation of water discharge

Water discharge was estimated by dividing the cross-channel topographic profile in 4 sections to calculate the water area (A_{water}) (Figure 15). For this, the estimated geometric area (A_{geo}) was subtracted from the core area (A_{core}) for each section. Then, the water discharge per section was calculated by multiplying A_{water} and the depth-averaged velocity current measured by the Aquadopps for the respectively section. Finally, the water discharge of the four sections was summed. The cross-channel topographic profile was interpolated with a distance interval of 0.1 m to extract representative water level with the side bank reaching an elevation of 4.85 m TAW (i.e. high water level). Also, the depth-averaged velocity current and water level was averaged every 30 min for the campaign period. Here, we assume that the current velocity measured by the Aquadopps at a specific location is representative for the velocity of the entire section while it is likely to be lower near the channel bank. Due to the limitation of the GPS profile coverage, extended elevations aligned with the profile were extracted from the LiDAR survey on 29/10/2019. Appendix A presents the extended profile and a map overlapping of the Qboat, GPS and LiDAR surveys. It was thus assumed that the sand bank did not change between October and December. The topographic elevation was compared between the GPS and Qboat in this appendix. Also, records from Aqd B were used in the water discharge estimation when there was any records from Aqd A due to the absence of water at its location.
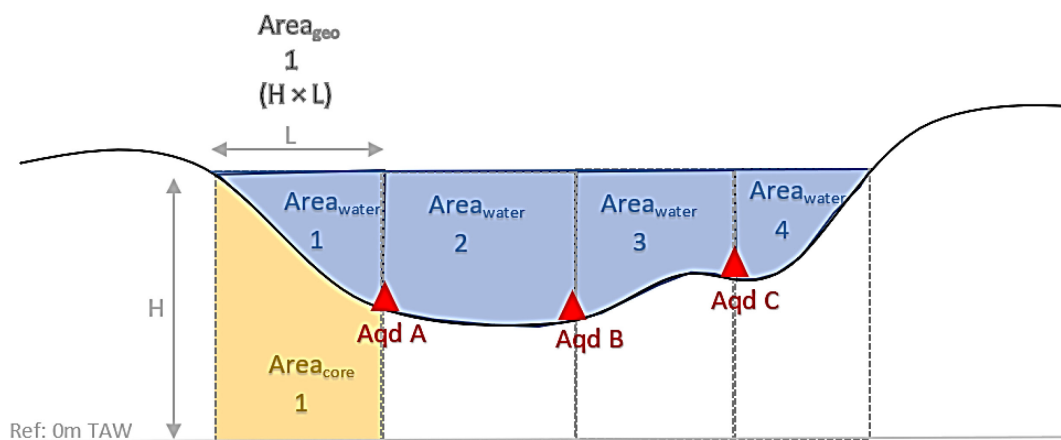
Figure 15 – Method of estimating water discharge.

E. SEDIMENT

Bed sediment samples were collected near the three Aquadopps. Grain size and carbonate content were analysed in the laboratory.

4.2.5   Results

A. Cross-channel topography

Figure 16 presents the cross-channel topographic profile acquired on 5/12. This profile was aligned with the Aquadopp sensors located in the channel and south of the permanent poles (Figure 12). The elevation in the channel was usually above 2 m TAW. The centre of the channel at a distance from 30 to 60 m was characterized by an elevation > 2.3 m TAW, which was higher than its sides. The east bank is characterized by a gentle intertidal slope while the west bank was steep and high (not surveyed due to a technical problem of receiving satellite signal).
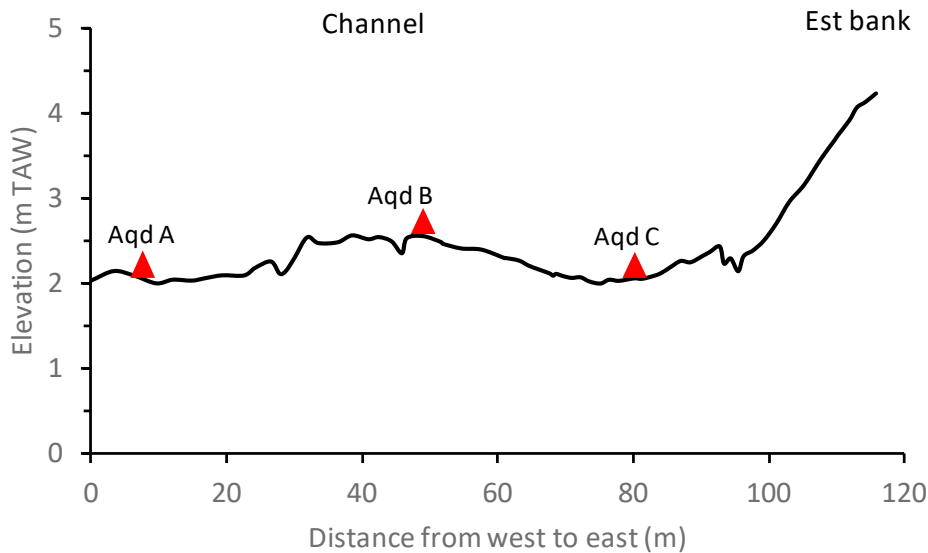
Figure 16 – Cross-channel topographic profile with the Aquadopp locations.

B. Current characteristics

Time series of velocity and direction profiles of the three Aquadopps are reported in Figure 17, Figure 18 and Figure 19. Also, velocity and direction depth-averaged values are presented there. As expected, the current velocity above 1.3 m from the bed was slightly faster than close to the bed where the shear effect limits the currents (i.e. a difference of at least 0.14 m/s).

Aqd A – west side of the channel
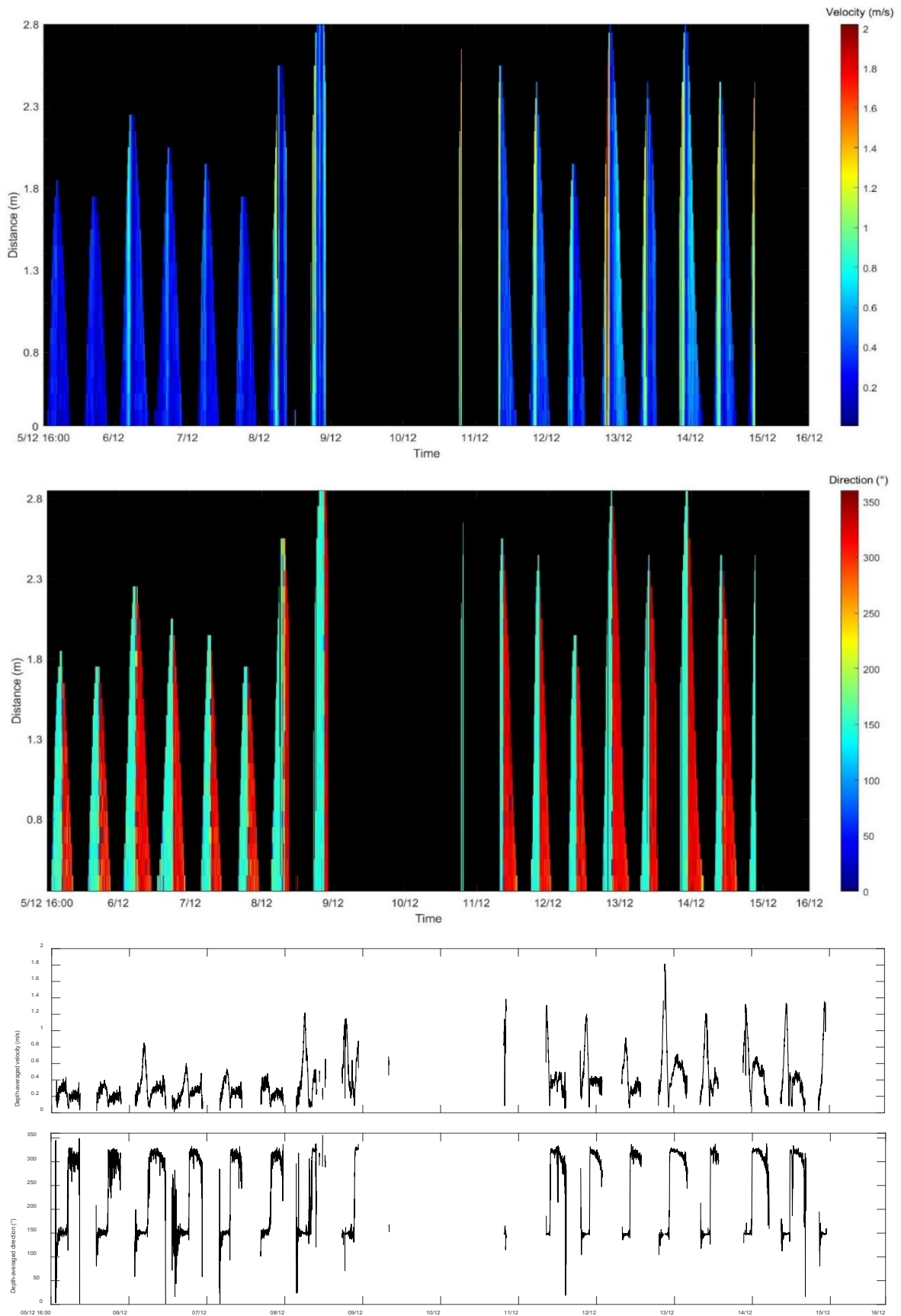
Figure 17 – Time series of current velocity profile, direction profile, and depth-averaged values for the Aquadopp A.
Note: Gaps in the time series are due to missing data.

Aqd – B centre of the channel
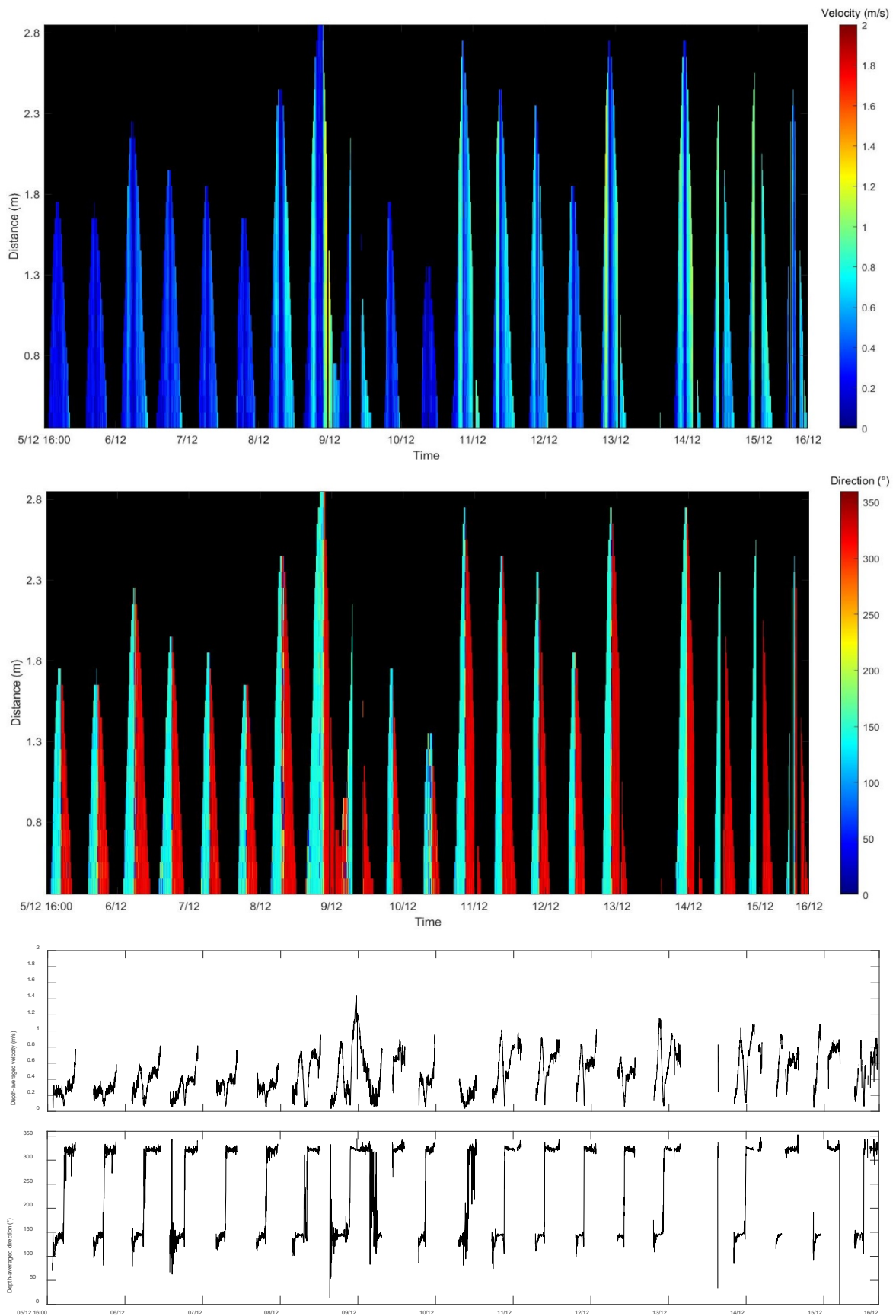
Figure 18 – Time series of current velocity profile, direction profile, and depth-averaged values for the Aquadopp B. Note: Gaps in the time series are due to missing data.

Aqd C- east side of the channel
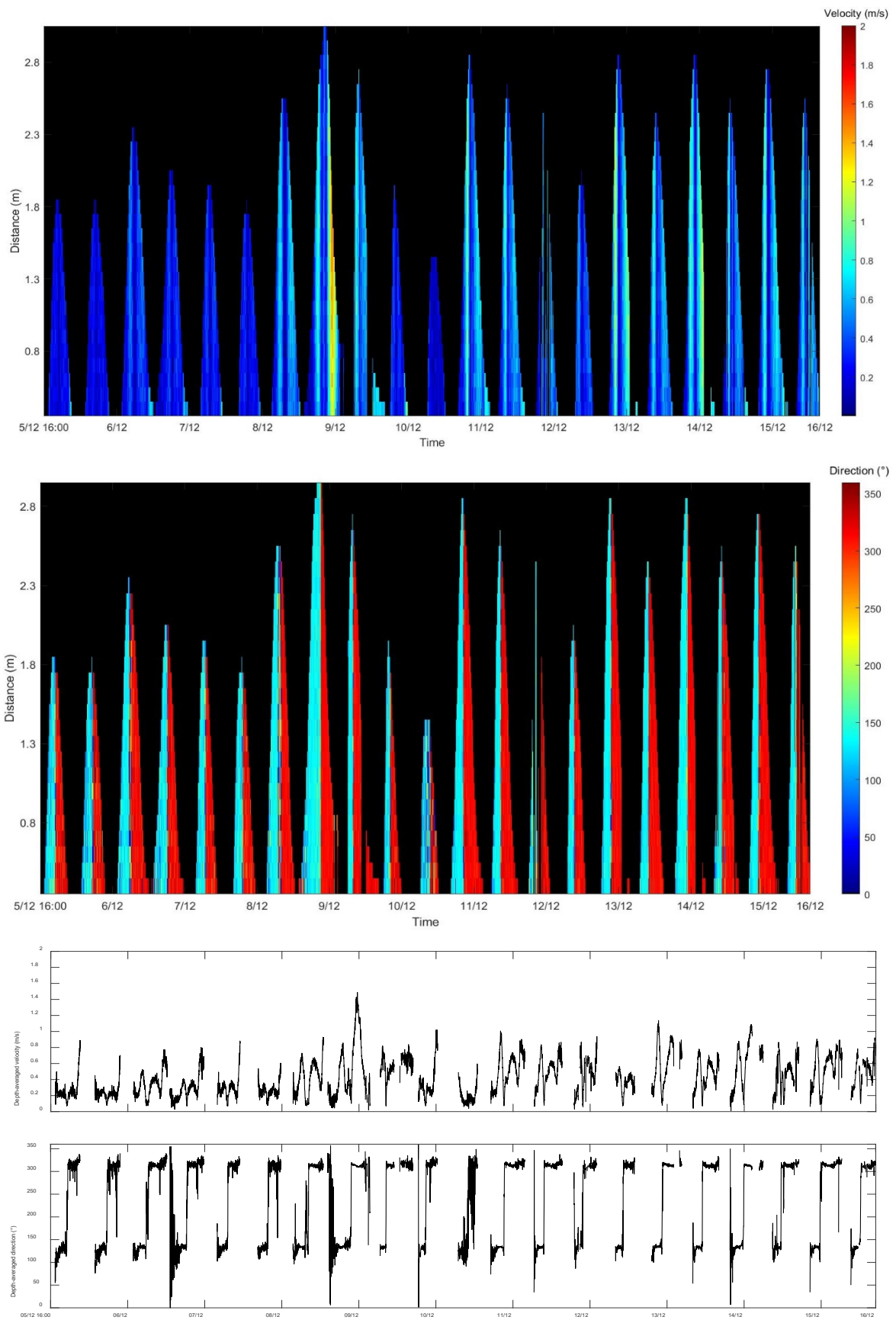
Figure 19 – Time series of current velocity profile, direction profile, and depth-averaged values for the Aquadopp C. Note: Gaps in the time series are due to missing data.

The three current roses clearly indicate an asymmetry of the tidal tide (Figure 20). The trend of Aqd B and Aqd C is very similar with a dominance of NW currents (310°) characterized by a maximum speed up to 1.4 m/s. This indicates that the current outflow is faster than the inflow there, suggesting that the east side and the middle of the channel are ebb-dominated (Figure 21). This process is similar to the entrance of the inlet (Montreuil et al., 2020). In contrast, the current rose of Aqd A shows a dominance of SE currents (150°) so that the inflow is the strongest there. Thus, the west side of the channel is flood dominated which is due to the local configuration with the presence of the sand bank and the steep west bank. These features are probably steered the tidal currents (i.e. secondary topographic effect). The segmentation of the sand bank morphology and its orientation of 175° (ebb-dominated) reflect this process as well.

Aqd A

Aqd B

Aqd C
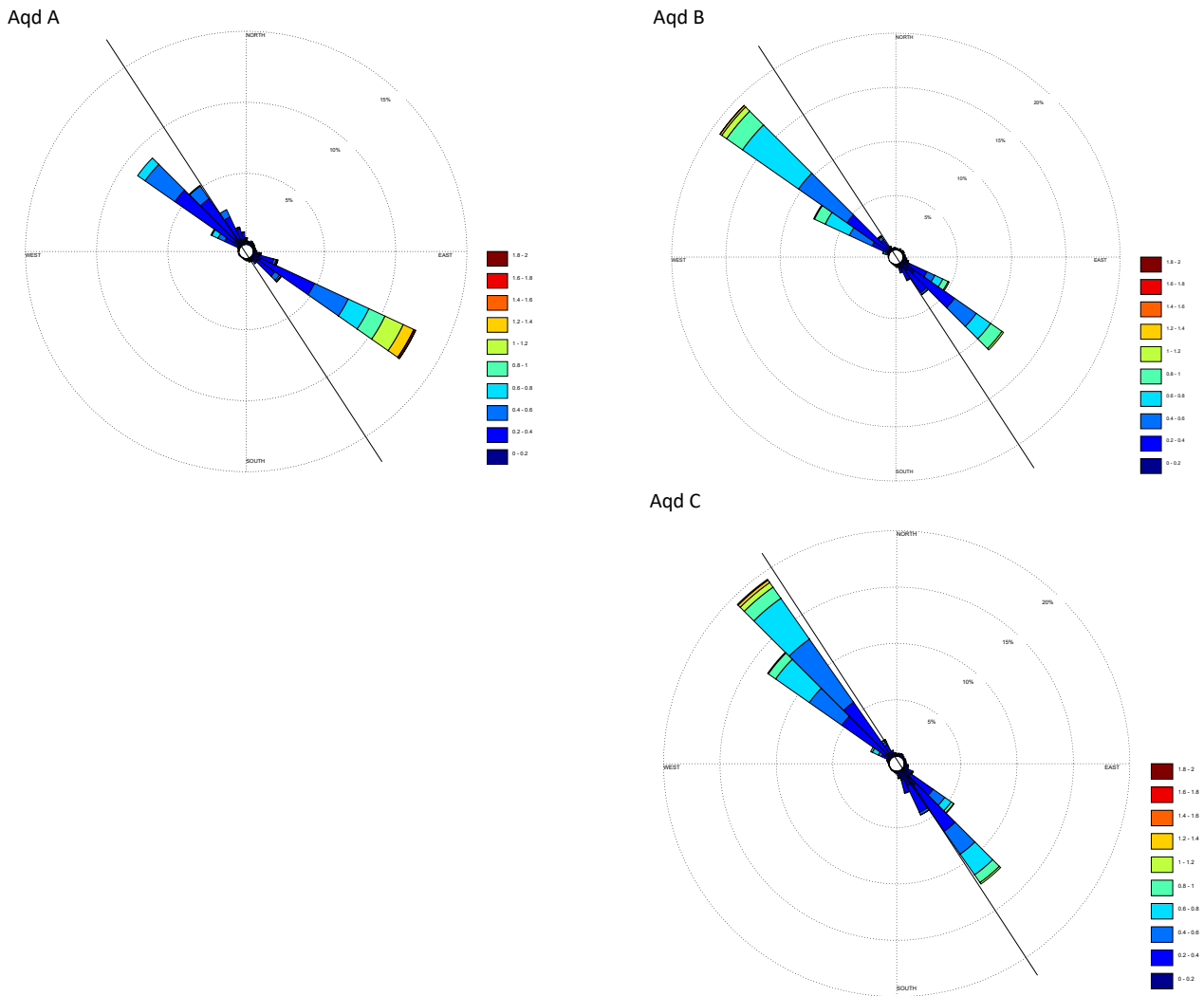
Figure 20 – Roses of current velocity (m/s) from the 3 Aquadopps.
Black lines correspond to the main channel orientation (130°-310°).
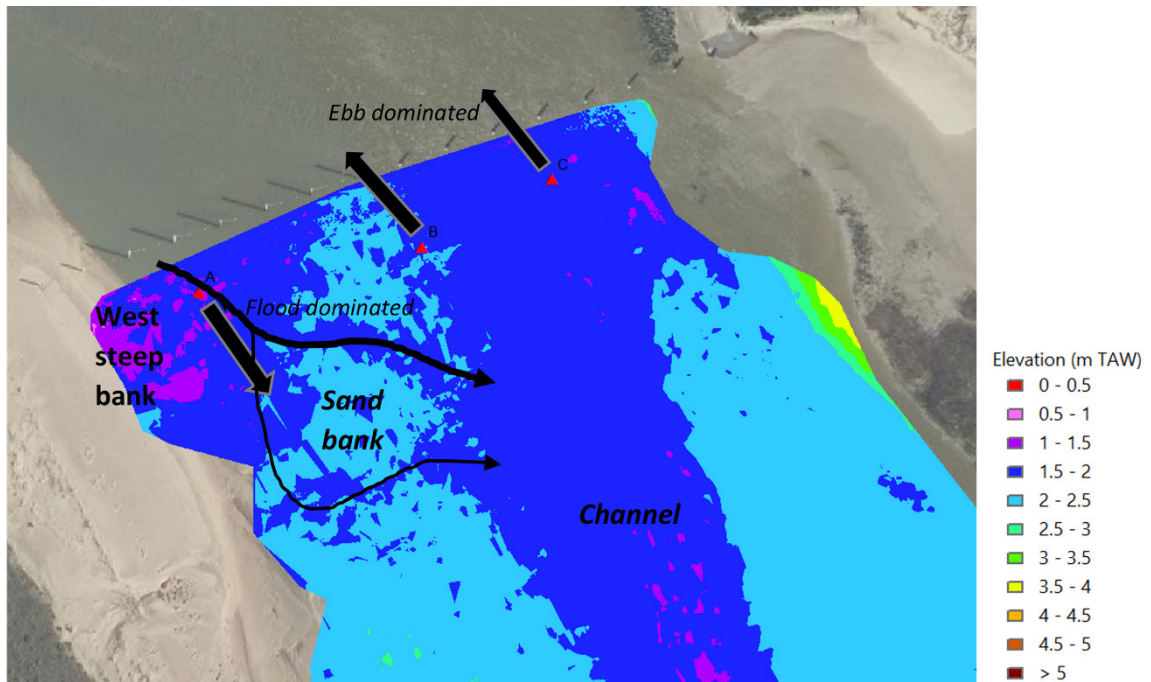
Figure 21 – Sketch of processes in the inland inlet.

C. Waves

The average of significant wave height was of 0.024 m with a maximum of 0.2 m during the entire campaign (Figure 22 and Table 13). Wave period was below 3.5 s which is lower than the typical values recorded along the coast (5-6 s). Also, wave direction was subject to a high variability, which might be biased and not representative.
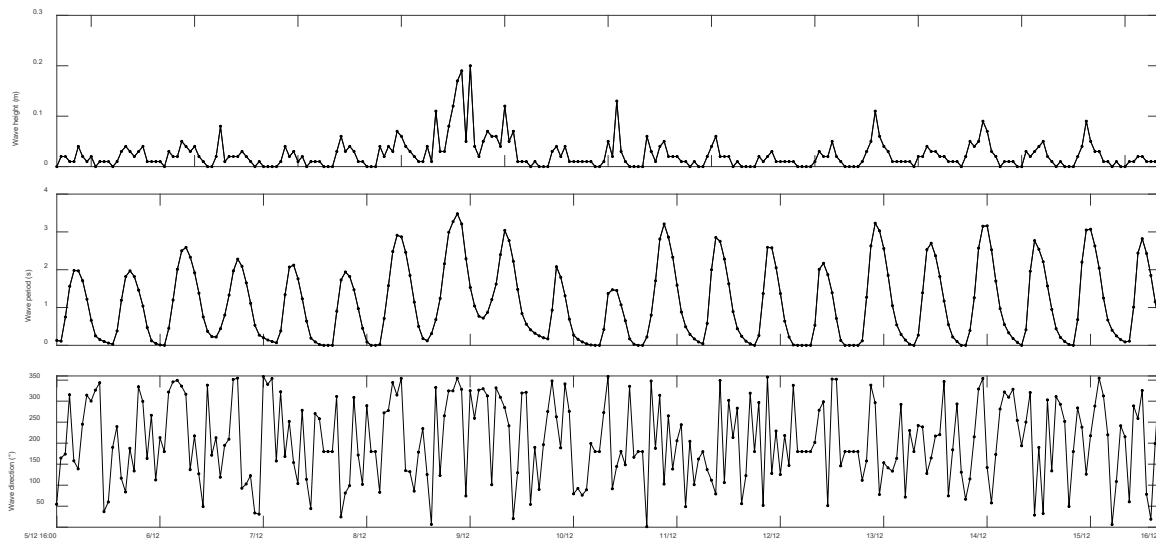
Figure 22 – Time series of significant wave height (Hm0), period (Tm0) and direction at the Aquadopp B.

Table 13 – Statistics summary of wave parameters.

Statistics	Hm0 (m)	T (s)	Dir (°)
Avg	0.024	1.097	204.865
Max	0.200	3.480	358.700

D. Water discharge

Aqua Vision carried out a survey with a controlled Q-boat 1800RP system (Aqua Vision, 2020) on 11-12/12/2019. Bathymetry and flow velocities were measured in the same cross-section as where the Aquadopps were deployed. Data were stored simultaneously and then controlled with ViSea Data Acquisition and survey toolbox softwares. Then these allowed to determine the water discharge.

The water discharge from the Qboat survey was determined at a specific location from the bathymetry and water velocity data throughout the water column. The velocity is measured in the middle of the profile and is extrapolated over the vertical (taken as representative). The measurement time window at each specific location ranged from 1 to 3 min. However, the transect was not completed no extrapolation was carried out for the sandbank sides of the channel. Also, the transects started from the seaward to landward so that the topography of some parts of the channel was missed. A comparison between results from the extrapolation and raw measurements collected on 12/12 was carried out by Aqua Vision (not presented here). The difference of water discharge estimation was negligible.

Figure 23 presents time series of water level and estimated water discharge from the Qboat and Aquadopps measurements. The time series called "average Aquadopps" (Avg Aqds) correspond to the water discharge estimations based on 30 minutes average current velocity and corresponding water level measurements, while "instantaneous Aquadopps" (Instant Aqds) are the immediate measurements of current velocity and water level measurements in the entire water column with an interval of 30 minutes. The results show the same pattern for the three types of water discharge time series. However, the Qboat estimation is systematically higher at high tide compared to the Aquadopps ones. A peak of 325.73 m^3 was found for the Qboat at high tide, while it was 259.99 m^3 and 265.3625 m^3 respectively for Instant and Average Aquadopp. The difference is probably due to the Qboat water discharge estimated at a specific point and not along the whole transect and without extrapolation for the side banks. Another reason for the difference of water discharges may be the difference of the bed topography (average 0.5 m) along the cross-section between the Qboat survey on 11-12/12 and the GPS measurements on 5/12 (Appendix A). These results are in agreement with the comparison of water discharge determined Qboat and 12 Aquadopps deployed across the channel in the inlet entrance on 25/10/2018 (Aqua Vision, 2018).
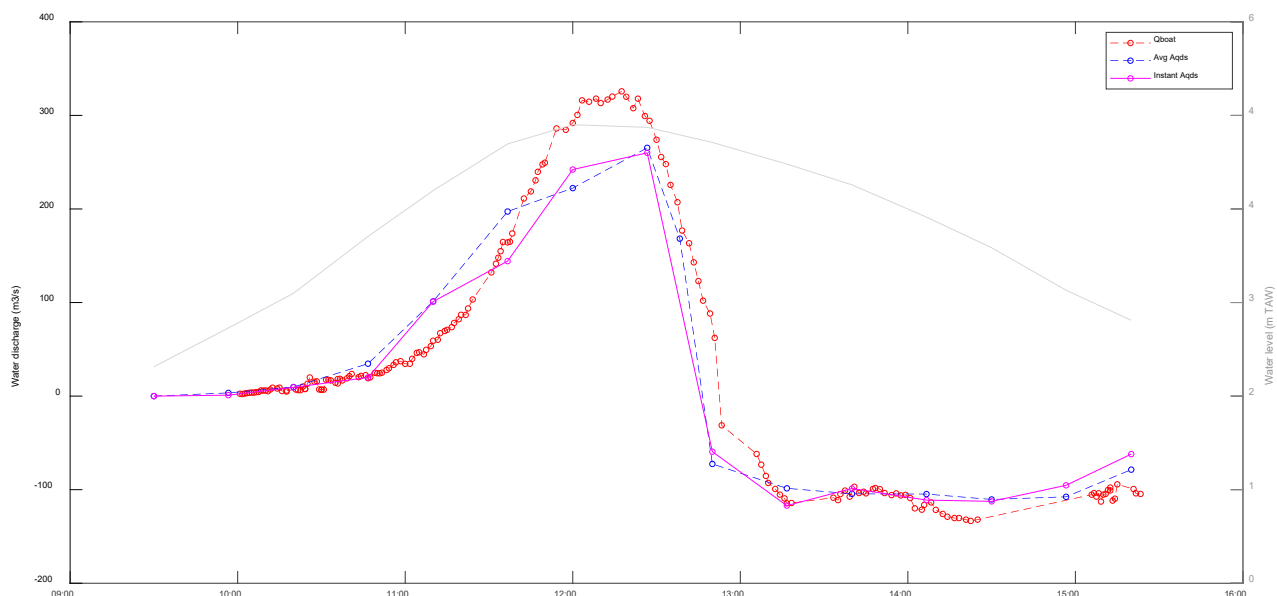
Figure 23 – Comparison of time series of water level (grey line) and estimated water discharge on 11/12/2019.

E. Sediment characteristics

The particle size of the sediment taken from the bottom at the 3 Aquadopp locations is presented in - Statistic summary of the grain size and carbonate content of the three sediment samples.Table 14. The sediments are quite homogenous at the 3 locations which consist of coarse sand with a D_{50} from 335 to 367 μm. These are nearly two times smaller than the sediment in the entrance inlet (Montreuil et al., 2020). The carbonate content ranges from 4.08 and 5.88 % which suggests a low content of shell fragments in the inland inlet.

Table 14 – Statistic summary of the grain size and carbonate content of the three sediment samples.

Sample	Grain size (μm)							Carbonate content (%)
	d (0.1)	d (0.2)	d(0.350)	d (0.5)	d(0.650)	d (0.8)	d (0.9)	
Aqd A	222.59	254.76	295.09	334.971	380.37	441.06	505.74	4.08
Aqd B	256.18	289.25	329.75	369.127	413.40	471.91	533.78	5.40
Aqd C	254.42	287.39	327.75	367.042	411.25	469.77	531.69	5.88

4.2.6 Hydrodynamic processes

A. Comparison water level in the inlet and at the coast

The water level recorded by the three Aquadopps based on their internal pressure sensors were referenced to TAW by adding the elevation of their position. Then they were compared to the Scheur monitoring station (Figure 24). The erroneous data below 2 m TAW were removed from the times series of the Aquadopps. The same pattern reflecting the tidal cycles was observed for the four sensors of recorded data. The water level records from AqdB and AqdC were nearly identical while they were slightly lower (<0.10 m) for Aqd A. The reason is probably due to a bias of the topographic measurement close to the west side bank where the satellite reception quality was poor.

Figure 24 – Comparison of the water level recorded in the inlet and at the coast from Scheur station.
Records at low water from the Aquadops were removed.

4.2.7   Conclusions

The second ad-hoc measurement in the Zwin was carried out from 5 to 16/12/2019 during a neap-spring tide period in the inland 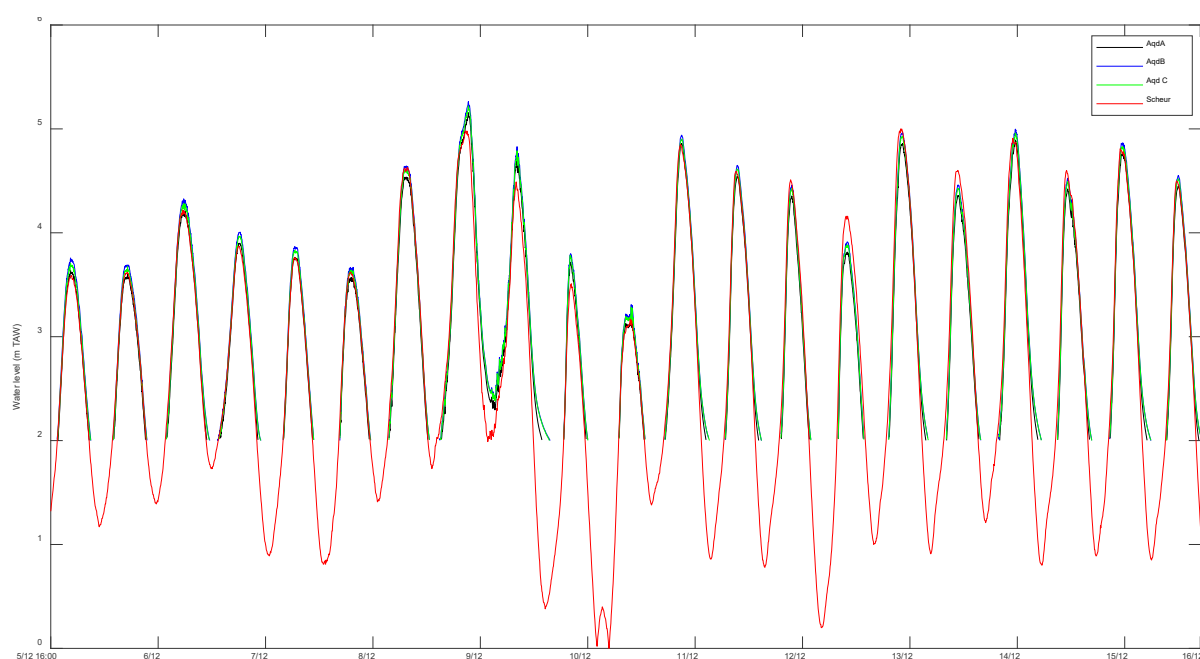inlet. The duration of the campaign was of 10 days and 17 hours covering 21 flood and ebb phases covering both calm and energetic conditions. Hydrodynamics were measured at three locations covering the east, center, and west side of the channel. Hydrodynamics in the centre (Aqd B) and east (Aqd C) of the channel are relatively similar with a slight dominance of NW (ebb) currents (310°) characterized by an average of 0.4-0.5 m/s and maximum speed up to 1.4 m/s. This indicates that the current outflow is faster than the inflow. Thus, a similar ebb-dominance to the one in the entrance of the inlet (Montreuil et al., 2020) is observed. The inflow is the strongest and directed SE (150°) at the west side of the channel. Thus, the flood-dominated process occurs probably caused by the presence of the sand bank and the steep west bank. These features might diffract currents (i.e. secondary diffracting effect). The morphological shape of the sand bank morphology and its orientation of 175° (ebb-dominated) reflects this process as well.

- Comparison of hydrodynamics state for 6 hours (a tidal phase from 2 hours before and 4 hours after high tide) indicates that the current velocity in the inland inlet ranges from 0.06 to 0.91 m/s under calm condition while it could be up to two times higher under energetic condition. In general, the strongest current velocity occurred 2 hours before high tide for the three Aquadopps while it is the lowest at high tide under both conditions. After high tide, the currents velocity progressively increases.

- From 2h before high tide, the current generally goes SE, while it is directed to W and NW 1h and 2h after high tide respectively. The difference of the current direction of the three Aquadopps is generally relatively low between calm and energetic condition (< 10° except for Aqd A and Aqd C 1h after high tide). Thus the current direction across the channel seems to be relatively unaffected by the hydrodynamic state as well the turning of the tide (around 20-30 min after high tide). Results suggest that the tidal reverse under energetic conditions occur around 20 min after high tide, while it takes more time, around 30 min, under calm conditions. Further measurements need to be carried out to confirm this hypothesis.

- The average of significant wave height was 0.024 m with a maximum of 0.2 m in the inland inlet during the entire campaign. Therefore, waves travelling in the inland inlet are restricted as well as transformed due to the shallowness of the area. Caution for uncertainty on measurement conditions must be made.

- Water discharge has been estimated by averaging data over an interval of 30 min across the channel from the 3 Aquadopps. The total volume of water that flowed in with the flood currents was around 400 m^3 in neap tide under typical hydrodynamic condition.

- The sediment consists of sand ranging from D_{50} from 335 to 367 µm. The carbonate content is relatively low at the 3 locations (< 6 %).

5 Discussion

5.1 Morphodynamics of the inlet

The results indicate that the entire Zwin inlet, characterized by a main channel, sandy bedforms of banks and bars, and gullies is a three-dimensional dynamic system. After more than one year from the dyke opening on 04/02/2019, significant morphological changes have occurred in the entrance channel of the inlet. Spatial and temporal morphological changes are observed with alternating accretion and erosion zones parallel to the coast as well as earn the edge of the salt marsh and dune line. This footprint is typical of migrating of three dimensional pattern and interplay between sandy bedforms and channel evolution. Based on the topographic cross-shore profiles, the channel is now nearly 0.7 m deeper (equivalent to a decrease of 0.03 m), up to 90 m wider and its thalweg migrated eastward compared to the pre-opening period. The combination of wave-induced and tidal currents are the main forcing factors driven morphological changes of the entrance inlet. Although there is a high spatial and temporal variability of the mobility of the sandy bedforms, the sediment volume is relatively stable in the entrance inlet unit since the opening of the dyke.

Moreover, remarkable morphological changes shaping the inland inlet unit have also occurred over the 1.9 years after the opening of the dyke. Two opposite morphodynamic trends occur in the inland inlet, with a sediment gain westward, while erosion dominates in the east and middle of the survey area where a net eastward shifting of the channel has occurred. Nearly 80 % of the inland inlet experiences erosion. It has thus been subject to a decrease of sediment volume equivalent to a reduction in bed height by 0.42 m over the monitoring period. As observed in the entrance inlet, the channel has become deeper, by a vertical amount exceeding 1 m at some locations. An increase of its width and migration toward the east reflect its behaviour and evolution. The narrow width of the inland channel is likely to accelerate the velocity of tidal currents which in turn induce erosion. In contrast, the west side of the inland inlet is accreting with the development of sand banks. They were supplied by sediment from the entrance inlet. This might explain the relative stability of the sediment budget there versus the material input from the sandy bedforms entering the inlet. This suggests interactions between the entrance and inland inlet units. Furthermore, the development of sand banks and their dynamics most probably influence the evolution of the channel. Bowman (1993) reported that the interactions between topography and tide hydraulics explain the spatial complexity of the channel and bedforms in the Zwin as well as their textural trends ranging from coarse sediment grain size and shell deposits in the entrance to fine sediment in the inland inlet.

As expected after the expansion of the surface area to over 333 ha, the entire inlet has changed, responding to both hydrodynamic and morphological feedback. Under the increase of the storage area of the inlet, the access channel adjusts by becoming wider and deeper in order to be able to drain larger volumes of water. As observed in the field, pronounced topographic forcing and steering occur during peak ebb and flood phase. This is clearly distinct in the north of the inland inlet where the curvature of the channel is high. In October 2020, the erosion rate of the east side of the inland inlet has decreased. Also, the main channel seems to have been increasingly transformed into a large tidal channel without any smaller branches/meanders. It can be hypothesized that the morphological changes inside the inlet might be largest just after the intervention work but will gradually diminish until they reach a dynamic equilibrium. Further topographic monitoring is needed to validate this hypothesis.

5.2 Water discharge and tidal prism

Flow rates in the main channel of the inland inlet recorded during the Qboat surveys before the opening of the dyke and 10/2020 are displayed in Figure 25 and Table 15. It is clear that the water discharge patterns have changed, characterized after opening by a longer flood phase of 2h30 with a flow peak of 171 m³ while it was just 1h45 in 10/2018 with a flow peak of 106 m³. In 10/2020, the estimated total water volume entering during the flood phase is of 6000 m³ which is two times larger than before the opening of the dyke. The ebb flow starts 45 min after high water (no change over the monitoring period). It rises rapidly to the maximum flow rates and then gradually decreases. In comparison with the records in 10/2018, the magnitude of the ebb flow rate ranges from 1.6 to 3 times higher in 10/2020. Despite the expansion of the channel area, the ebb phase still lasts longer than the flood phase. It results in a tidal asymmetry with faster flood flow rates than the ebb ones. This can result in the system silting up (tidal pumping) and in particular in those areas where the current is less concentrated and its velocity decreases rapidly over a short distance. The inlet is a flood-dominated system subject to a dynamic behaviour and fast evolution.
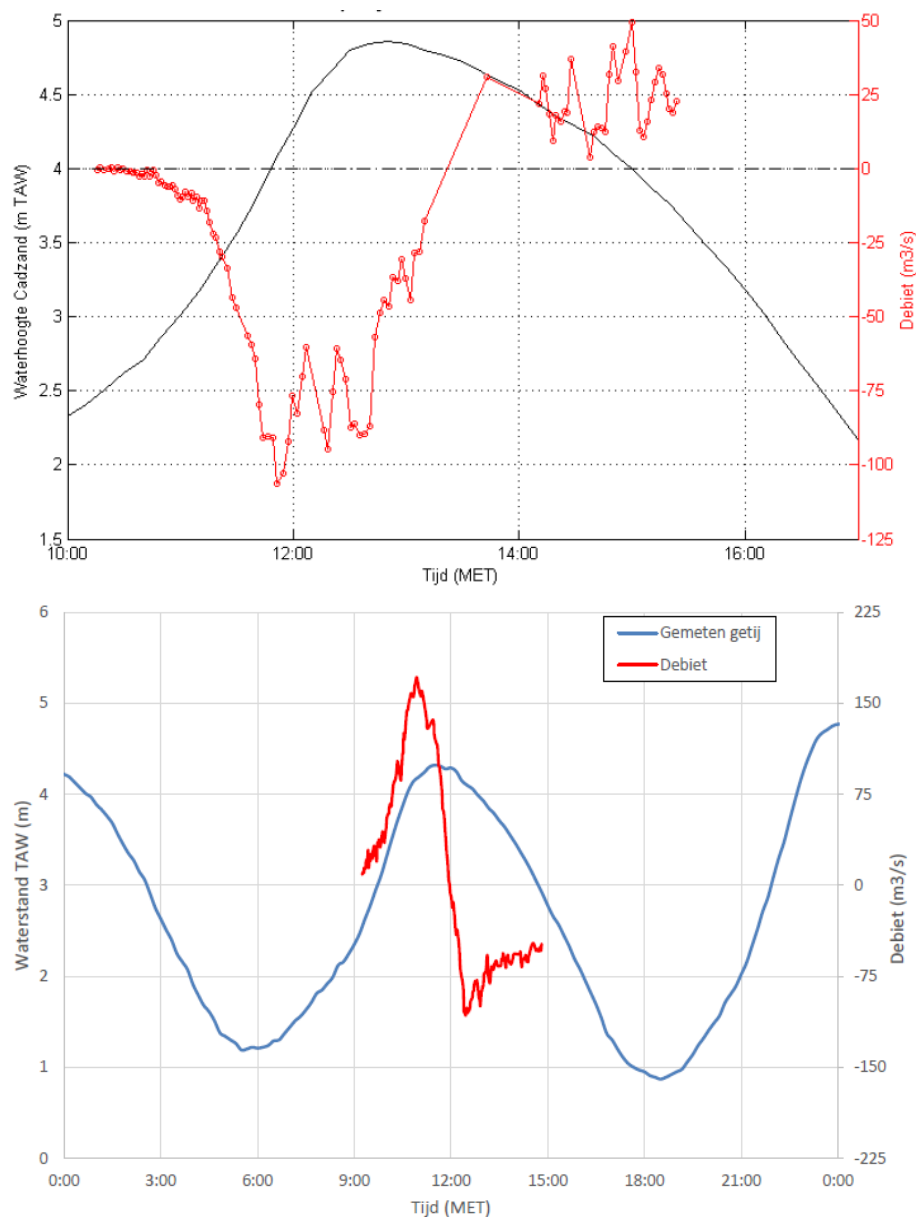

Figure 25 – Comparison of water discharge and water level for the Qboat surveys on 23/10/2018, before the opening of the dyke (top) and 28/10/2020 (bottom) (Aqua Vision, 2018, 2020b).

Table 15 – Summary of water discharge in the inland inlet based on the Qboat surveys.

	Flood discharge			Ebb discharge			High water level (m TAW)
	Mean (m³/s)	Max (m³/s)	Total (m³)	Mean (m³/s)	Max (m³/s)	Total Total (m³)	
10/07/2017	32	114	1483	-17	-28	-700	4.5
18/12/2017	36	106	2912	-21	-40	-855	4.64
11/04/2018	18	54	1907	-10	-21	-779	4.02
11/07/2018	28	99	1903	-15	-29	-1305	4.32
23/10/2018	38	106	2901	-23	-49	-772	4.73
01/02/2019	/	/	/	/	/	/	/
06/03/2019	68	176	5176	-77	-90	-2625	4.34
17/06/2019	99	228	8701	-77	-116	-5221	4.38
16/09/2019	83	270	7398	-99	-141	-4855	4.61
11/12/2019	97	326	11722	-106	-133	-5929	4.4
04/06/2020	43	310	7463	-114	-151	-10974	4.78
29/09/2020	40	196	2342	-88	-116	-6042	4.58
28/10/2020	63	171	6000	-67	-107	-5633	4.24

Note: No water discharge was recorded in 02/2019 due to bad atmospheric conditions limiting the number of ship tracks to estimate it.

The tidal prism is defined as the amount of water that flows in and out of the tidal inlet during one tidal period. The tidal prism influences the cross-sectional area, the stability of the main inlet channel and controls the intertidal flat area. To estimate the tidal prism, the water basin area is determined, assuming that water levels are uniform within the basin. The tidal prism is derived as (O'Brien, 1969):

$$Tidal\ prism = \int_{Zmin}^{Zmax} water\ basin\ area\ (z)dz$$

where *Zmax* and *Zmin* is the maximum and minimum water level within a tidal period respectively. This definition is equal to the volume determined by the intersection of the Zmax plane with the topography and the topographic surface surveyed during Zmin.

In this study, the water basin area was determined using the LiDAR DEMs covering both the entrance and inland inlet units at three dates: pre-dyke opening (06/11/2018), 2.5 month after opening (20/04/2019) and 14 months after opening (10/04/2020). The water basin area and volume were determined as a function of water level assuming that water levels are uniform throughout the basin. Since the LiDAR system does not penetrate water, it turns out to be less accurate in the channel. Based on a survey error of 3 cm in the vertical direction, the estimated volume error for a spring water level is below 9770 m³. Figure 26 presents the water basin area and volume as a function of water level (i.e. hypsometry) for the entrance inlet and inland inlet units. As expected, linear relationships are generally found between the area, the respective volume, and the water level. Noteworthily, the water basin area of the inland inlet strongly increases between 3 and 3.5 m TAW which might be explained by the flooding of the tidal flats. Also, the results show that the tidal prism that enters in the Zwin is highly dependent on the maximum water level reached during the tidal cycle. Under spring conditions (4.7 m TAW), the estimations of the water basin volume at the entrance inlet and inland inlet units are 508 881 m³ and 205 262 m³ respectively (based on DEMs) on 10/04/2020. During storm conditions, the combination of surge and high tide is likely to increase the tidal prism for the entire inlet. This

needs to be further investigated. After 1.2 year of the opening of the dyke, the water basin area and volume of both inlet units have gradually enlarged. Specifically, an increase of basin volume exceeding 8.3 % and 26.5 % have occurred for the entrance and inlet respectively. A growth of the tidal prism thus enhances the drainage of the inlet which gradually reduce the silting up process. An increase of tidal prism could lead to a reduction of the development of sandy bedforms (Oost, 1992). This would suggest that the decrease of the tidal prism of the Zwin might favour the disappearance of the sand bars and banks along the channel. Further investigations needs to be done to confirm this hypothesis.
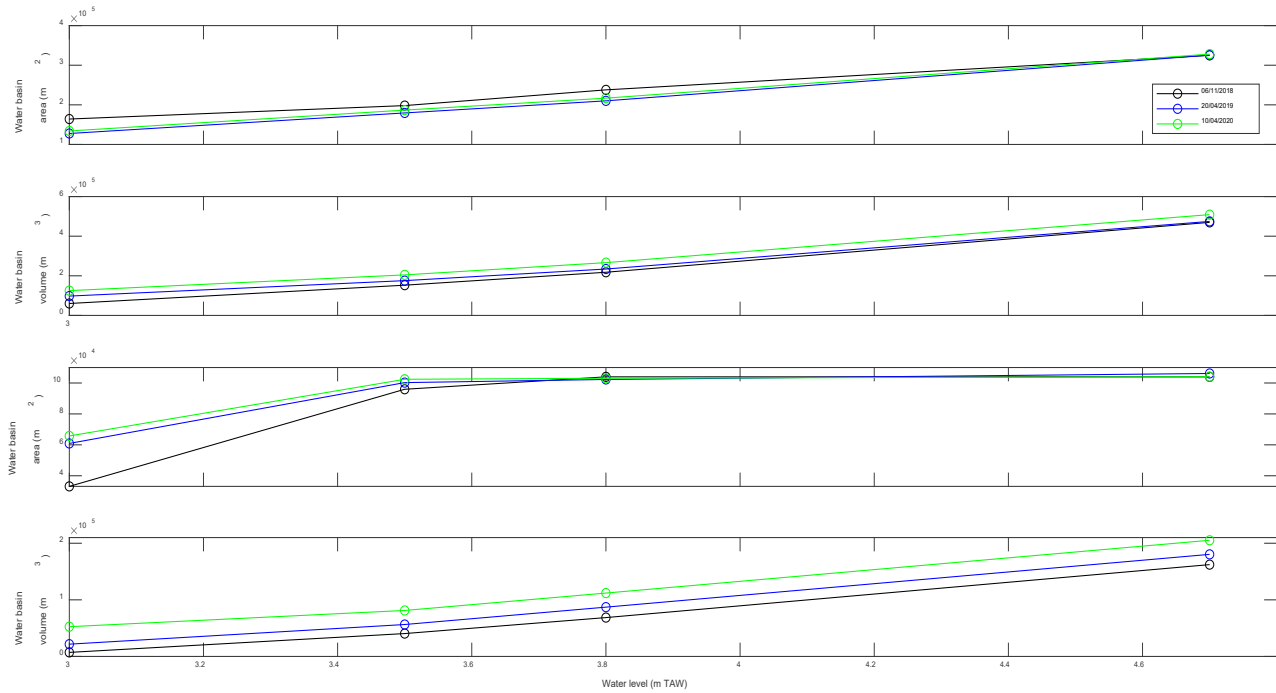

Figure 26 – Hypsometry of the entrance inlet (first two panel) and inland inlet (last two panel) as a function of water level. Note the difference of y-axes.

6 Conclusions

The Zwin tidal inlet is a complex morphological system functioning as a continuous interaction between the hydrodynamic forces (waves, tides) and the local topography and it is strongly influenced by the sediment supply variability, the tidal prism (the volume of water exchanged with the sea during a tidal cycle) and the local ecology. This study reports the morpho- and hydrodynamics of the entire tidal inlet from the situation pre-opening (dike removal on the 4th of February 2019) up to 1.9 month post-opening.

Immediately after the expansion of the intertidal area by over 333 ha, the inlet reacted mainly by changing the local topography/bathymetry. The main tidal channel adjusted progressively by becoming wider and deeper in order to be able to drain larger volumes of water. After one year the volume of water exchanged with the sea increased up to 11 %. This trend continued in the second year when the water increased by 8.3 % and 26.5 % for the entrance and inland inlet unit respectively (period 06/11/2018-10/04/2020 and based on the spring high water level). In the first year the channel deepened by 0.5 m and widened to 18 m, while approximately two years after the opening, the significant morphological changes increased in the channel of the entrance unit, seaward of the inlet, which became nearly 0.7 m deeper and up to 90 m wider.

The combination of wave-induced and tidal currents is the main forcing factor driving morphological changes of the entrance inlet. The relative stability of the sediment volume in the entrance contrasts with the overall erosion of the inland inlet. The inland inlet unit experiences remarkable morphological changes by losing large volumes of sediment, with deepening exceeding 1 m at some locations after the opening of the dyke. Additionally, the channel widening is associated with an eastward migration. However, the west side of the inland inlet is in an accretionary state with the development of sand banks. Probably, this is caused by a sediment supply from the entrance inlet indicating clear interaction between the units.

In addition, the water discharge patterns have changed over the monitoring period. After the first year, the difference of water discharge for the flood and ebb phases was in average up to 45 m^3/s and 74 m^3/s larger than before the pre-opening volumes. After two years, the flood phase which lasts 45 minutes longer and a 1.6 times faster flow peak. In October 2020, the estimated total water discharge during the flood flow was 6000 m^3 which is two times larger than the pre-opening situation. The water discharge during ebb flow has also increased. The water discharge is characterized by a smooth transition with a clear cyclic pattern between tidal phases. It is probable that the morphological changes inside the Zwin inlet were maximal during the first few months after the intervention works and it can be expected that they will then gradually diminish until reaching a dynamic equilibrium. The continuation of the monitoring is recommended in order to confirm the observed trends and to improve the scientific understanding of the hydrodynamic processes driving the morphological response in the Zwin inlet as well as its long-term evolution.

7   References

Aqua Vision (2018) Het Zwin Bathymetrie en stromingsmetingen oktober 2018, 25p.

Aqua Vision (2019) Het Zwin Bathymetrie en stromingsmetingen juni 2019, 25p.

Aqua Vision (2020a) Het Zwin Bathymetrie en stromingsmetingen september 2020, 23p.

Aqua Vision (2020b) Het Zwin Bathymetrie en stromingsmetingen oktober 2020, 23p.

Montreuil, A-L., Dan, S., Verwaest, T., Mostaert, F. (2020) Monitoring the morphodynamics of the Zwin inlet: interim report: 1 year after the works. Version 0.1. FHR Reports, 16_89_1. Flanders Hydraulics Research: Antwerp.

Bowman, D. (1993) Morphodynamics of the stagnating Zwin inlet, The Netherlands, Sedimentary Geology, 84, 219-239.

O'Brien, M.P. (1969) Equilibrium flow areas of inlets on sandy coasts. Journal of Waterway Port Coast Ocean Engineering 95 (1) 43-52.

Oost, A.P. (1992) Sedimentological implications of the closure of the Lauwersea and the developmebnt of the Frisian inlet system. 3rd International Research Symposium of Modern and Ancient Clastic Tidal Depositis, Wilhelmshaven, 107.

Van der Vegt, M., Hoekstra, P. (2012) Morphodynamics of a storm-dominated, shallow tidal inlets: the Slufter, the Netherlands. Netherlands Journal of Geosciences, 991-3, 325-339.

Appendix – GPS, Qboat and LiDAR surveys for water discharge estimation, profile and map
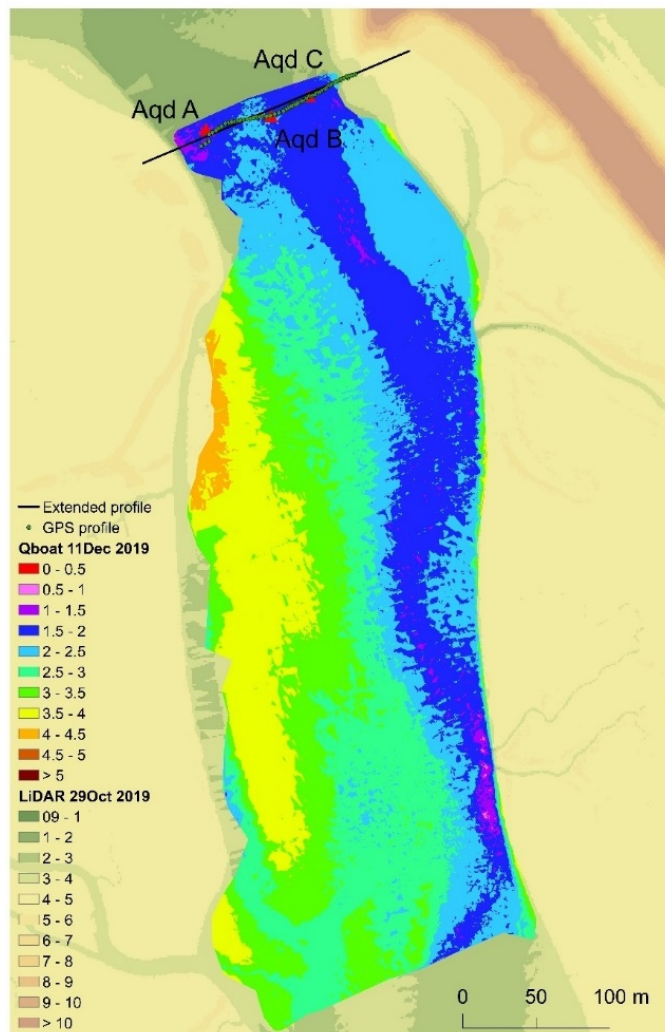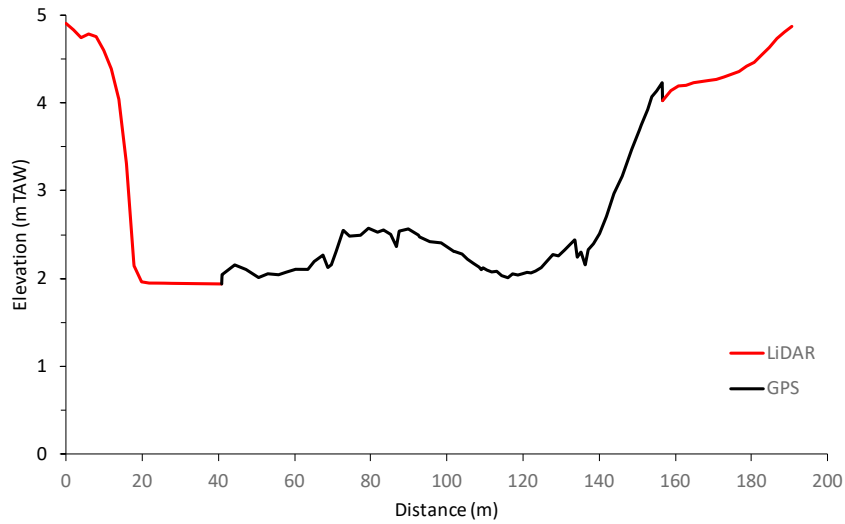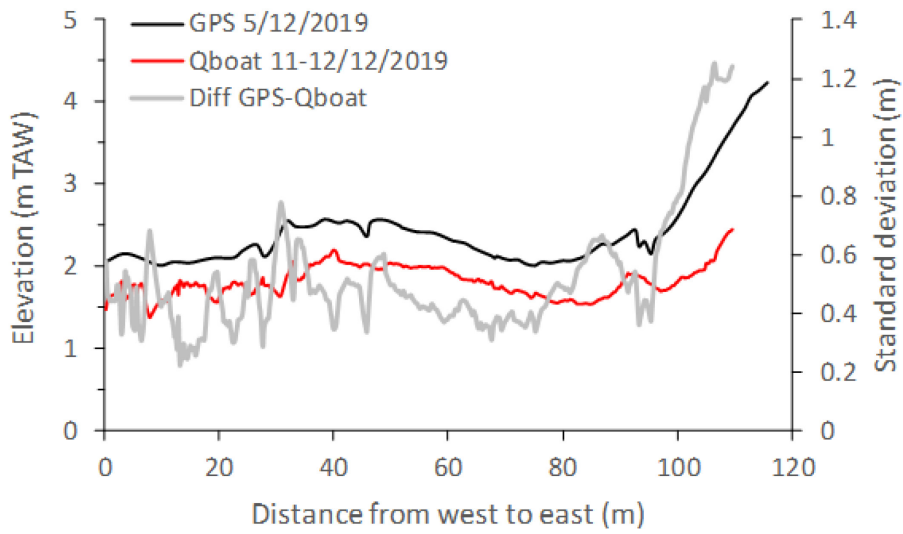
Difference between the GPS and Qboat survey:

Elevation difference (m)	
Mean	0.53
Max	1.25
Min	0.22
SD	0.21

The Qboat and GPS surveys were recorded at the same time so that elevation change could have happened between the period. Also, the error associated with the respective system could also explain the difference.